
Efficient and Generalizable Certified Unlearning: A Hessian-free Recollection Approach

Xinbao Qiao¹

Meng Zhang²

Ming Tang³

Ermin Wei⁴

^{1,2}Zhejiang University, ³Southern University of Science and Technology, ⁴Northwestern University
xinbao.22@intl.zju.edu.cn

Abstract

Machine unlearning strives to uphold the data owners' right to be forgotten by enabling models to selectively forget specific data. Recent advances suggest pre-computing and storing statistics extracted from second-order information and implementing unlearning through Newton-style updates. However, the theoretical analysis of these works often depends on restrictive assumptions of convexity and smoothness, and those mentioned operations on Hessian matrix are extremely costly. As a result, applying these works to high-dimensional models becomes challenging. In this paper, we propose an efficient Hessian-free certified unlearning. We propose to maintain a statistical vector for each data, computed through affine stochastic recursion approximation of the difference between retrained and learned models. Our analysis does not involve inverting Hessian and thus can be extended to *non-convex non-smooth* objectives. Under same assumptions, we demonstrate advancements of proposed method beyond the state-of-the-art theoretical studies, in terms of generalization, unlearning guarantee, deletion capacity, and computation/storage complexity, and we show that the unlearned model of our proposed approach is close to or same as the retrained model. Based on the strategy of recollecting statistics for forgetting data, we develop an algorithm that achieves *near-instantaneous* unlearning as it only requires a vector addition operation. Experiments demonstrate that the proposed scheme surpasses existing results by orders of magnitude in terms of time/storage costs, while also enhancing accuracy.

1 Introduction

Recent data protection regulations, e.g. General Data Protection Regulation, aim to safeguard individual privacy. These regulations emphasize the provisions of the *Right to be Forgotten*, which grants individuals the ability to request the removal of personal data. This regulation mandates that the data controller shall erase personal data without undue delay when data providers request to delete it. Within the context of the right to be forgotten, data owners can request the removal of their personal data's contribution from trained models. This can be achieved through the concept of *machine unlearning*, which involves erasing data that pertains to the data owner's personal information.

A straightforward unlearning algorithm is to retrain a learned model from scratch, which is however impractical as it comes with unaffordable monetary and time costs. It is especially challenging in time-sensitive applications such as fraud detection or online learning, as neglecting timeliness may have a detrimental impact on system performance and responsiveness. Moreover, attaining a model entirely identical to the one achieved through retraining for an unlearning method represents a notably demanding criterion. Therefore, many approximate methods have been proposed aiming to minimize the impact of forgetting data. Inspired by differential privacy, [1] introduced a relaxed definition of certified unlearning, which aims to make unlearned model indistinguishable from retrained model.

Table 1: d is the dimensionality of the model parameters, and n is the total size of the dataset.

Methods	Pre-computation time	Storage	Unlearning time (per sample)
Sekhari <i>et al.</i> [2]	$\mathcal{O}(nd^2)$	$\mathcal{O}(d^2)$	$\mathcal{O}(d^3)$
Suriyakumar <i>et al.</i> [3]	$\mathcal{O}(d^3 + nd^2)$	$\mathcal{O}(d^2)$	$\mathcal{O}(d^2)$
Proposed Hessian-free method	$\mathcal{O}(nd)$	$\mathcal{O}(nd)$	$\mathcal{O}(d)$

Second-order unlearning methods have been recently studied due to their rigorous unlearning certification and the generalization guarantee. Sekhari *et al.* [2] initially proposed Newton update method and introduced the definition of deletion capacity to understand the relationship between generalization performance and the amount of deleted samples. These method and concepts were later extended, e.g. [3, 4, 5, 6]. The key idea of these works is to extract Hessian information of the loss function and achieve computational and memory efficiency by pre-computing and storing these second-order statistics prior to any deletion request. In particular, Sekhari *et al.* [2] and Suriyakumar *et al.* [3] studies reveal that for models that approximate the minimization of convex and sufficiently smooth empirical minimization objectives, unlearning can be efficiently executed through a Newton style step, facilitated by pre-storing Hessian matrix. While these works have demonstrated the effectiveness of second-order method to approximate retrained model with limited updates, they do have a few fundamental limitations. First, most existing certified unlearning algorithms require the explicit pre-storage of the Hessian matrix (or its inverse) and are hence expensive to implement, especially in high-dimensional models. This forms a stark contrast to many algorithms leveraging Hessian-free solvers, e.g. exploit the Hessian vector product technique [7] without explicitly computing Hessian matrix. Second, their analyses are not applicable to most deep neural networks due to their requirement of convexity assumption. We are thus motivated to answer the following key question:

How to realize certified unlearning without directly computing Hessian and restrictive assumptions?

In contrast to prior works, this paper aims to study the efficient second-order unlearning methods from a new Hessian-free perspective. Specifically, we analyze the difference between the learned and retrained models for each sample by recollecting the trajectory discrepancy. Subsequently, we demonstrate that these discrepancies can be approximated and characterized through an affine stochastic recursion. We summarize our main contributions related to theoretical and experimental results below, and the contributions related to algorithm efficiency in Table 1.

- **Hessian-Free Analysis.** We propose a method to extract Hessian information by analyzing each sample’s impact on the training trajectory without explicitly computing the Hessian. Our method allows us to leverage the Hessian-free technique, which enjoys better scalability compared to existing second-order unlearning methods. Since our analysis avoids inverting Hessian, it can also be extended to *non-convex non-smooth* objectives. To our best knowledge, our work is the first to establish non-convex theoretical analysis of certified unlearning. (Section 3).
- **Improved Guarantees and Complexity.** We demonstrate advancements of proposed method compared to the state-of-the-art theoretical studies, in terms of generalization (See Theorem Theorem 5), unlearning guarantee (See Theorem 4), deletion capacity (See Theorem 8), and computation/storage complexity (See Subsection 4.4 and Table 1). Especially in Theorem 4, we show the proposed method can almost achieve the same model as the retrained model. (Section 4).
- **Instantaneous Unlearning Algorithm.** Building upon the aforementioned analysis, we develop a Hessian-free unlearning algorithm. To our best knowledge, our algorithm is *near-instantaneous* and currently the most efficient as it only requires a vector addition operation. (Section 4).
- **Comprehensive Evaluation.** We conduct experimental evaluations using a wider range of metrics compared to previous theoretical studies for certified unlearning. The experimental results verify our theoretical analysis and demonstrate that our proposed approach surpasses previous certified unlearning works. In particular, our algorithm incurs the millisecond-level unlearning runtime to forget per sample with minimal performance degradation. (Section 5).

1.1 Related Work

Machine unlearning can be traced back to [8] and their work defines the notion of completeness, demanding that the models obtained through retraining and unlearning exhibit complete consistency.

Exact Unlearning methods, e.g., [9, 10, 11, 12, 13, 14], train submodels based on different dataset partitions and aggregation strategies (See detailed exact unlearning background in [Appendix A](#)). **Approximate Unlearning**, e.g. [15, 16, 17, 18, 19, 20, 21, 22, 23, 24, 25] seeks to minimize the impact of forgetting data to an acceptable level to tradeoff for computational efficiency, reduced storage costs, and flexibility (See detailed approximate unlearning background in [Appendix A](#)). In particular, [1] introduced a relaxed (ϵ, δ) -certified unlearning definition, in anticipation of ensuring the output distribution of the unlearning algorithm is indistinguishable from that of the retraining. Building upon this framework, diverse methodologies, e.g. [2, 3, 4, 6, 26, 27], have been devised.

In the certified unlearning definition, the Hessian-based approaches [2, 3, 4] are aligned with our methodology, which involves pre-computing data statistics that extract second-order information from the Hessian matrix, and utilizing these precomputed ‘recollections’ to facilitate data forgetting. Specifically, (1) **Newton Step (NS)**. [2] proposes, through the precomputation and storage of the Hessian offline, to achieve forgetting upon the arrival of a forgetting request using a Newton step. However, this method necessitates strong assumptions, e.g. the objective function is required to be strongly convex. Its unlearning time, involving $\mathcal{O}(d^3)$, becomes nearly impractical for over-parameterized deep neural networks. (2) **Infinitesimal Jackknife (IJ)**. [3, 4] extends the work of NS, attaining strong convexity through a non-smooth regularizer by leveraging the proximal IJ with reduced unlearning time $\mathcal{O}(d^2)$. However, the basic issues still exist, i.e., existing certified unlearning methods, especially those focused on establishing theoretical results, have largely focused on convex and smooth settings while requiring expensive Hessian matrix computations. On the contrary, our method provides a breakthrough for certified unlearning in a non-convex non-smooth setting. In addition, as indicated in [Table 1](#), our method breaks the curse of model parameters dimensionality. Moreover, prior works necessitate maintaining the Hessian (or its inverse) to address the ongoing deletion requests, which poses the risk of violating the right to be forgotten and entails user privacy. Instead, our method goes beyond ‘recollecting to forget’ by also ‘forgetting the recollections’.

2 Problem Formulation

Learning Let $\ell(\mathbf{w}; z)$ be the loss function for a given parameter $\mathbf{w} \in \mathbb{R}^d$ and on instance z over an instance space \mathcal{Z} . Learning can be expressed as the population risk minimization problem:

$$\min_{\mathbf{w}} F(\mathbf{w}) := \mathbb{E}_{z \sim \mathcal{D}}[\ell(\mathbf{w}; z)]. \quad (1)$$

Addressing this problem directly is challenging, as the probability distribution \mathcal{D} is usually unknown. For a finite dataset $\mathcal{S} = \{z_i\}_{i=1}^n$, one often solves the following empirical risk minimization problem:

$$\min_{\mathbf{w}} F_{\mathcal{S}}(\mathbf{w}) := \frac{1}{n} \sum_{i=1}^n \ell(\mathbf{w}; z_i). \quad (2)$$

A standard approach to solve the problem (2) is the stochastic gradient descent (SGD), iterating towards the direction with stepsize η of the negative gradient (stochastically):

$$\mathbf{w}_{e,b+1} \leftarrow \mathbf{w}_{e,b} - \frac{\eta_{e,b}}{|\mathcal{B}_{e,b}|} \sum_{i \in \mathcal{B}_{e,b}} \nabla \ell(\mathbf{w}_{e,b}; z_i), \quad (3)$$

for the index of epoch update $e \in \{0, \dots, E\}$ and the index of batch update $b \in \{0, \dots, B\}$, where E is total epochs and B is batches per epoch. Here, $\mathcal{B}_{e,b}$ denotes the dataset that contains the data sampled in the e -th epoch’s b -th update, and $|\mathcal{B}_{e,b}|$ is the size of $\mathcal{B}_{e,b}$, where $|\mathcal{B}|$ is the maximum batchsize.

Unlearning Consider a scenario where a user requests to remove a forgetting dataset $U = \{u_j\}_{j=1}^m \subseteq \mathcal{S}$. To unlearn U , retraining from scratch is considered a naive unlearning method, which aims to minimize $F_{\mathcal{S} \setminus U}(\mathbf{w})$. Specifically, since each sample takes place only in one (mini-)batch per epoch, we define the data point u_j in U to be sampled in $\mathcal{B}_{e,b(u_j)}$ during the e -th epoch’s $b(u_j)$ -th batch update in the learning process, where $b(u_j)$ represents the batch update index when u_j is sampled. Due to the removal of sample u_j , the batch $\mathcal{B}_{e,b(u_j)}$ is reduced to $\mathcal{B}_{e,b(u_j)} \setminus \{u_j\}$. In accordance with the linear scaling rule discussed in [28], i.e., in order to effectively leverage batch sizes, one has to adjust the stepsize in tandem with the batch size. The retraining stepsize thus is concurrently scaled to $\eta_{e,b(u_j)} \frac{|\mathcal{B}_{e,b(u_j)} \setminus \{u_j\}|}{|\mathcal{B}_{e,b(u_j)}|}$. Therefore, the retraining update rule in e -th epoch is given by,

$$\mathbf{w}_{e,b+1}^{-U} \leftarrow \mathbf{w}_{e,b}^{-U} - \frac{\eta_{e,b}}{|\mathcal{B}_{e,b}|} \sum_{i \in \mathcal{B}_{e,b}} \nabla \ell(\mathbf{w}_{e,b}^{-U}; z_i). \quad (4)$$

Specifically, for the data point u_j sampled into $\mathcal{B}_{e,b}$ during e -th epoch's $b(u_j)$ -th update, we have:

$$\mathbf{w}_{e,b(u_j)+1}^{-U} \leftarrow \mathbf{w}_{e,b(u_j)}^{-U} - \frac{\eta_{e,b(u_j)}}{|\mathcal{B}_{e,b(u_j)}|} \sum_{i \in \mathcal{B}_{e,b(u_j)} \setminus \{u_j\}} \nabla \ell(\mathbf{w}_{e,b(u_j)}^{-U}; z_i). \quad (5)$$

To avoid the unaffordable costs incurred by the retraining algorithm, we aim to approximate the retrained model through limited updates on the learned model $\mathbf{w}_{e,b+1}$. We thus consider the relaxed definition of model indistinguishability defined by Sekhari et al. [2].

Definition 1 ((ϵ, δ) -certified unlearning). *Let S be a training set and $\Omega : S \rightarrow \mathbf{w}$ be an algorithm that trains on S and outputs a model $\mathcal{T}(S)$ represent the additional data statistics that need to store (typically not the entire dataset). Given an output of learning algorithm $\Omega \in \mathcal{W}$ and a set of data deletion requests U , we obtain the results of the unlearning algorithm $\bar{\Omega}(\Omega(S), \mathcal{T}(S)) \in \mathcal{W}$ and the retraining algorithm $\bar{\Omega}(\Omega(S \setminus U), \emptyset)$ through a removal mechanism $\bar{\Omega}$. For $0 < \epsilon \leq 1$ and $\forall \mathcal{W} \subseteq \mathcal{R}^d, S \subseteq \mathcal{Z}$, we say that the removal mechanism $\bar{\Omega}$ satisfies (ϵ, δ) -certified unlearning if*

$$\begin{aligned} \mathbb{P}(\bar{\Omega}(\Omega(S), \mathcal{T}(S)) \leq e^\epsilon \mathbb{P}(\bar{\Omega}(\Omega(S \setminus U), \emptyset))) + \delta, \text{ and} \\ \mathbb{P}(\bar{\Omega}(\Omega(S \setminus U), \emptyset) \leq e^\epsilon \mathbb{P}(\bar{\Omega}(\Omega(S), \mathcal{T}(S))) + \delta. \end{aligned} \quad (6)$$

3 Main Intuition and Solution Justification

Before detailing our analysis, let us informally motivate our main method. Specifically, we focus on studying the discrepancy between the learning and the retraining model by analyzing the impact of each sample on the update trajectory. Our main observation is that the difference between the retraining and learning models analyzed through SGD recursion, can be described by an *affine stochastic recursion*. See full proofs of Section 3 in Appendix B.1 and Appendix B.2.

Unlearning a single data sample. We start with designing an approximator for a single sample (i.e., $U = \{u\}$) on the training updates (the learning update and retraining update), by considering the difference between the learning model in (3) and the retraining model obtained without the knowledge of u in (4). In particular, we consider the following two cases of model updates in the e -th epoch.

Case 1 (u not in $\mathcal{B}_{e,b}$): The difference between retraining and learning updates in the e -th epoch is

$$\mathbf{w}_{e,b+1}^{-u} - \mathbf{w}_{e,b+1} = \mathbf{w}_{e,b}^{-u} - \mathbf{w}_{e,b} - \frac{\eta_{e,b}}{|\mathcal{B}_{e,b}|} \sum_{i \in \mathcal{B}_{e,b}} \left(\nabla \ell(\mathbf{w}_{e,b}^{-u}; z_i) - \nabla \ell(\mathbf{w}_{e,b}; z_i) \right). \quad (7)$$

From the Taylor expansion of $\nabla \ell(\mathbf{w}_{e,b}^{-u}; z_i)$ around $\mathbf{w}_{e,b}$, we have $\nabla \ell(\mathbf{w}_{e,b}^{-u}; z_i) = \nabla \ell(\mathbf{w}_{e,b}; z_i) + \nabla^2 \ell(\mathbf{w}_{e,b}; z_i)(\mathbf{w}_{e,b}^{-u} - \mathbf{w}_{e,b}) + o(\mathbf{w}_{e,b}^{-u} - \mathbf{w}_{e,b})$. Let $\mathbf{H}_{e,b} = \sum_{i \in \mathcal{B}_{e,b}} \nabla^2 \ell(\mathbf{w}_{e,b}; z_i)$ denote the Hessian of the loss during the e -th epoch's b -th update, we can then approximate the SGD recursion (7) as

$$\mathbf{w}_{e,b+1}^{-u} - \mathbf{w}_{e,b+1} \approx \left(\mathbf{I} - \frac{\eta_{e,b}}{|\mathcal{B}_{e,b}|} \mathbf{H}_{e,b} \right) (\mathbf{w}_{e,b}^{-u} - \mathbf{w}_{e,b}). \quad (8)$$

Case 2 (u in $\mathcal{B}_{e,b(u)}$): The difference between retraining and learning updates in the e -th epoch is:

$$\mathbf{w}_{e,b(u)+1}^{-u} - \mathbf{w}_{e,b(u)+1} \approx \underbrace{\left(\mathbf{I} - \frac{\eta_{e,b(u)}}{|\mathcal{B}_{e,b(u)}|} \mathbf{H}_{e,b(u)} \right)}_{\text{Approximate impact of } u \text{ in previous epoches}} (\mathbf{w}_{e,b(u)}^{-u} - \mathbf{w}_{e,b(u)}) + \underbrace{\frac{\eta_{e,b(u)}}{|\mathcal{B}_{e,b(u)}|} \nabla \ell(\mathbf{w}_{e,b(u)}; u)}_{\text{Approximate impact of } u \text{ in epoch } e}, \quad (9)$$

where \mathbf{I} denotes identity matrix of appropriate size. Combining the observations in Cases 1 and 2, we now define the *recollection* matrix $\mathbf{M}_{e,b(u)}$ and affine stochastic recursion approximator $\mathbf{a}_{E,B}^{-u}$, backtracking the overall difference between the retrained model and the learned model:

$$\mathbf{a}_{E,B}^{-u} := \sum_{e=0}^E \mathbf{M}_{e,b(u)} \nabla \ell(\mathbf{w}_{e,b(u)}; u), \quad \mathbf{M}_{e,b(u)} := \frac{\eta_{e,b(u)}}{|\mathcal{B}_{e,b(u)}|} \prod_{k=e}^E \prod_{b=b(u)+1}^{B-1} \left(\mathbf{I} - \frac{\eta_{k,b}}{|\mathcal{B}_{k,b}|} \mathbf{H}_{k,b} \right). \quad (10)$$

We will see that $\mathbf{a}_{E,B}^{-u}$ can approximate the impact of sample u on the training trajectory¹ as follows,

$$\mathbf{w}_{E,B}^{-u} - \mathbf{w}_{E,B} \approx \mathbf{a}_{E,B}^{-u}, \quad (11)$$

¹Similar analysis has been conducted in other lines of work to investigate the behavior of SGD dynamics, e.g. reference [29] focused on the properties of the matrix $\mathbf{I} - \frac{\eta}{|\mathcal{B}|} \mathbf{H}$, which is termed as multiplicative noise, serving as the main source of heavy-tails in SGD dynamics and governing the update behavior of $\mathbf{w}_{e,b}$.

That is, a simple vector $\mathbf{a}_{E,B}^{-u}$ addition to model $\mathbf{w}_{E,B}$ can obtain an approximate retrained model for forgetting the sample u . We define $\Delta_{E,B}^{-u} = \mathbf{w}_{E,B}^{-u} - \mathbf{w}_{E,B} - \mathbf{a}_{E,B}^{-u}$ as the approximation error.

Our designed approximator in (10) enables us to exploit the Hessian vector product (HVP) technique [7] to compute it without explicitly computing the Hessian. When computing the product of the Hessian matrix and an arbitrary vector for the deep neural networks, the HVP technique first obtains gradients during the first backpropagation, multiplying the gradients with the vector, and then performing backpropagation again to obtain the results. This results in a time complexity of $\mathcal{O}(d)$. We note that the existing second-order methods require to proactively store a Hessian matrix (or its inverse) [2, 3, 4]. It is thus unable to deploy the HVP in their settings.

Note that our proposed analysis does not require to invert Hessian matrix, distinguishing it from existing Newton-like methods [2, 3, 4]. This eliminates the need for assuming strong convexity in order to ensure the invertibility of the Hessian. In our analysis, we consider the approximation error under general non-convex non-smooth settings (e.g., deep neural networks) by examining the spectral radius ρ of the recollection matrix $\mathbf{M}_{e,b(u)}$, which characterizes the discrepancy between the retrained and learned model $\mathbf{w}_{E,B}^{-U} - \mathbf{w}_{E,B}$. Moreover, when it comes to forgetting a set of samples, we have,

Theorem 1 (Additivity). *When m sequential deletion requests arrive, the sum of m approximators is equivalent to performing batch deletion simultaneously, i.e., for u_1, \dots, u_m sequence of continuously arriving deletion requests, we demonstrate that $\mathbf{a}_{E,B}^{-\sum_{j=1}^m u_j} = \sum_{j=1}^m \mathbf{a}_{E,B}^{-u_j}$.*

This elucidates that by storing the impact of updates for each sample, nearly instantaneous data removal can be achieved through a series of vector additions.

4 Theoretical Analysis and Algorithm Design

In this section, we first analyze the approximation error $\Delta_{E,B}^{-U}$ under non-convex non-smooth setting. We then demonstrate that under the same assumptions, our method can almost obtain an identical retrained model and achieve better unlearning guarantee and generalization results compared to previous theoretical unlearning works [2, 3, 4]. We further develop our proposed unlearning algorithm, which is one of the most efficient and nearly instantaneous. Finally, we provide storage/computation complexity analysis of proposed algorithm and show that it is more efficient compared to prior works.

4.1 Approximation Error Analysis

To analyze the approximation error $\Delta_{E,B}^{-U}$, we introduce the following lemmata. We first bound the approximation error through gradient clipping, which is widely adopted to achieve favorable performances in deep network training, by ensuring gradient norms are not excessively large [30]. We further show that the gradient clipping with geometrically decaying stepsizes also facilitates us to derive an upper bound for the remainder term $o(\mathbf{w}_{e,b}^{-u} - \mathbf{w}_{e,b})$ in the following:

Lemma 2. *In the learning stage, we threshold the stochastic gradient norm at C , i.e., $\|\nabla \ell(\mathbf{w}; z)\| \leq C$. To simplify the expression, we define that SGD performs a total of $t \in \{0, \dots, T\}$ steps for $\mathbf{w}_{e,b}$, where $t = eB + b$. Consider geometrically decaying stepsizes satisfying $\eta_{t+1} = q\eta_t$, where $0 < q < 1$ and $\eta = \eta_0$. Therefore, after t steps, for any forgetting set U , we have:*

$$\|\mathbf{w}_{e,b}^{-U} - \mathbf{w}_{e,b}\| \leq 2\eta C \frac{1 - q^t}{1 - q}. \quad (12)$$

See proof in Appendix B.3. Then we further analyze the properties of the Hessian matrix:

Lemma 3. *For all e, b and vector $\mathbf{v} \in \mathbb{R}^d$, assume that exists λ and M such that $\lambda \mathbf{I} \preceq \nabla^2 \ell(\mathbf{w}_{e,b}; z_i) \preceq M \mathbf{I}$, and let $\rho = \max\{|1 - \eta_{e,b}\lambda|, |1 - \eta_{e,b}M|\}$ be the spectral radius of $\mathbf{I} - \frac{\eta_{e,b}}{|\mathcal{B}_{e,b}|} \mathbf{H}_{e,b}$, we have $\|(\mathbf{I} - \frac{\eta_{e,b}}{|\mathcal{B}_{e,b}|} \mathbf{H}_{e,b}) \mathbf{v}\| \leq \rho \|\mathbf{v}\|$.*

Therefore, combining (10), Lemma 2 and Lemma 3, we have the following upper bound:

Theorem 4 (Unlearning Guarantee). *For any subset of samples $U = \{u_j\}_{j=1}^m$ to be forgotten, the unlearned model based on the approximator $\mathbf{a}_{E,B}^{-U}$ in (10) leads to an approximate error bounded by*

$$\|\Delta_{E,B}^{-U}\| = \|\mathbf{w}_{E,B}^{-U} - \mathbf{w}_{E,B} - \mathbf{a}_{E,B}^{-U}\| \leq 2\eta C \zeta_T^{-U}, \quad (13)$$

where T is the total number of update steps, and we define $\zeta_T^{-U} = \mathcal{O}\left(\frac{\rho^T - q^T}{\rho - q} - \frac{\rho^T - q^{2T}}{\rho - q^2} + \frac{\rho^T - q^T}{\rho^B - q^B}\right)$.

See proof in [Appendix B.4](#). Intuitively, [Theorem 4](#) shows that through stochastic matrix recursions of (8) and (9), the remainder terms $o(\mathbf{w}_{e,b}^{-u} - \mathbf{w}_{e,b})$ of the previous rounds are scaled by subsequent recollection matrices $\mathbf{M}_{e,b}$, and generate a new remainder term in this round, which is a polynomial multiply geometric progression. As a result, when $\rho < 1$ (e.g., [Assumption 1](#)), in a scenario where T is sufficiently large, the error tends towards zero. This implies that the unlearned model can nearly approximate the retrained model. Notably, it is worth mentioning that the upper bounds provided by previous theoretical works [2, 3, 4] are non-zero under [Assumption 1](#).

4.2 Generalization Properties Analysis

To discuss the performance guarantee of our proposed method, we further analyze the generalization performance. We present a generalization of the excess risk as defined in problem (1). Subsequently, we conduct an asymptotic analysis of our method, showing that for strongly convex and smooth objectives, our approach can asymptotically approach the retrained objective.

We adopt the following standard assumptions (e.g., similar to prior certified unlearning works [3, 4]):

Assumption 1. For any z and \mathbf{w} , the loss $\ell(\mathbf{w}; z)$ is λ -strongly convex, L -lipschitz and M -smooth.

Theorem 5 (Generalization Guarantee). Let [Assumption 1](#) hold. Choose $\eta \leq \frac{2}{M+\lambda}$, then we have $\rho < 1$. Let \mathbf{w}^* be the minimizer of the population risk in problem (1) and T be the total number of update steps. Considering the forgetting dataset U and an unlearned model $\tilde{\mathbf{w}}_{E,B}^{-U}$, we have following excess risk,

$$F(\tilde{\mathbf{w}}_{E,B}^{-U}) - \mathbb{E}[F(\mathbf{w}^*)] = \mathcal{O}\left(\frac{4L^2}{\lambda(n-m)} + \rho^T \frac{2L^2}{\lambda} + \frac{2L\eta C \sqrt{d} \sqrt{\ln(1/\delta)}}{\epsilon} \zeta_T^{-U}\right). \quad (14)$$

The proof is included in [Appendix B.6](#), where we perform an asymptotic analysis. Specifically, the result of our proposed method is expected to converge to $\mathcal{O}\left(\frac{L^2}{\lambda(n-m)}\right)$ as T approaches infinity. It is noteworthy that, under these conditions and the fact that $n = \Omega(m)$, our proposed approximator outperforms the performance of previous methods [2, 3, 4] which are greater than $\mathcal{O}\left(\frac{L^2}{\lambda(n-m)}\right)$. Furthermore, to measure the maximum number of samples to be forgotten while still ensuring good excess risk guarantees, we analyze the *deletion capacity* of our proposed scheme, similar as in [2]. Due to the space limit, we defer the definition and analysis to [Appendix E.1](#), where we compare our main theoretical results for generalization and deletion capacity with previous works.

4.3 Efficient Unlearning Algorithm Design

Based on the above methods and the analysis of [Theorem 4](#), we now propose a memory and computationally efficient unlearning scheme in [Algorithm 1](#). To our best knowledge, our method is currently one of the most efficient, as it only requires a single vector addition by utilizing offline computed statistics. Besides, our proposed algorithm also ensures complete forgetting by deleting the approximator of the corresponding sample post-unlearning, rather than storing such statistics.

We present our approach in [Algorithm 1](#). In **Stage I**, we bound approximation error through gradient clipping and perform model training normally. Upon completing the model training, we proceed to **Stage II**, where we compute the unlearning statistics vector $\mathbf{a}_{E,B}^{-u}$ for each sample u . To reduce computational complexity, we leverage the HVP technique. The computed approximators $\{\mathbf{a}_{E,B}^{-u_j}\}_{j=1}^n$ are then stored for further use. A deletion request initiates **Stage III**. In this stage, the indistinguishability of the (ϵ, δ) -unlearning guarantee, as defined in [Definition 1](#), is achieved through a single vector addition with injected noise. Notably, our unlearning approach does not necessitate accessing any datasets during Stage III. Moreover, in contrast to prior works that require retaining privacy-sensitive statistics to handle subsequent forgetting requests, our approach eliminates the need to retain statistics post-unlearning by simply discarding them. Lastly, our method necessitates minimal modifications to existing training frameworks. This characteristic renders our approach orthogonal to any training innovations and opens up possibilities for its future expansion, e.g., our method can be combined with fine-tuning to enhance performance. Specifically, this involves training on a small number of epochs with the remaining dataset, and then adding the corresponding approximators during this period to the original approximators. The detailed strategy is described in [Appendix E.3](#).

Algorithm 1: Hessian-free Online Unlearning (HF) Algorithm

```

1 Stage I: Learning model  $\mathbf{w}_{E,B}$  on dataset  $S = \{z_i\}_{i=1}^n$ :
2 for  $e = 0, 1 \dots, E$  do
3   for  $b = 0, 1 \dots, B$  do
4     Compute gradient:  $\mathbf{g} \leftarrow \frac{1}{|\mathcal{B}_{e,b}|} \sum_{i \in \mathcal{B}_{e,b}} \nabla \ell(\mathbf{w}_{e,b}; z_i) \times \max(1, \frac{C}{\|\nabla \ell(\mathbf{w}_{e,b}; z_i)\|})$ ,
5     Gradient descent:  $\mathbf{w}_{e,b+1} \leftarrow \mathbf{w}_{e,b} - \eta_{e,b} \mathbf{g}$ 
6   end
7 end
8 Stage II: Pre-computing and Pre-storing statistics  $\mathcal{T}(S) = \{\mathbf{a}_{E,B}^{-u_j}\}_{j=1}^n$ :
9 for  $j = 1, 2 \dots, n$  do
10   Recursive computation by using HVP:  $\mathbf{a}_{E,B}^{-u_j} \leftarrow \sum_{e=1}^E \mathbf{M}_{e,b(u_j)} \nabla \ell(\mathbf{w}_{e,b(u_j)}; u_j)$ ,
11   where  $\mathbf{M}_{e,b(u_j)} = \frac{\eta_{e,b(u_j)}}{|\mathcal{B}_{e,b(u_j)}|} \prod_{k=e}^E \prod_{b=b(u_j)+1}^{B-1} (\mathbf{I} - \frac{\eta_{k,b}}{|\mathcal{B}_{k,b}|} \mathbf{H}_{k,b})$ 
12 end
13 Stage III: Unlearning when user requests to forget the subset  $U = \{u_j\}_{j=1}^m$  on model  $\mathbf{w}_{E,B}$ :
14 Compute:  $\bar{\mathbf{w}}_{E,B}^{-U} \leftarrow \mathbf{w}_{E,B} + \mathbf{a}_{E,B}^{-U}$ ,  $c \leftarrow 2\eta C \frac{\sqrt{2\ln(1.25/\delta)}}{\epsilon} \zeta_T^{-U}$  Delete statistics:  $\{\mathbf{a}_{E,B}^{-u_j}\}_{j=1}^m$ 
15 Sample:  $\sigma \sim \mathcal{N}(0, c\mathbf{I})$ , Return:  $\tilde{\mathbf{w}}_{E,B}^{-U} = \bar{\mathbf{w}}_{E,B}^{-U} + \sigma$ 

```

4.4 Comparison to Existing Approaches

We provide a brief overview of previous second-order unlearning works and compare the complexity of our method with these works in terms of pre-computation, storage, and unlearning time.

Newton Step (NS). Sekhari et al. [2] proposed an efficient certified unlearning method by pre-storing the Hessian $\sum_{i=1}^n \nabla^2 \ell(\mathbf{w}_{E,B}; z_i)$. When a request arrives to forget m samples U , we obtain an unlearned model $\mathbf{w}_{E,B}^{-U}$ by adding the approximator $\mathbf{a}_{\text{NS}}^{-U}$ to original learned model $\mathbf{w}_{E,B}$.

$$\mathbf{a}_{\text{NS}}^{-U} = \frac{1}{n-m} \mathbf{H}_{\text{NS}}^{-1} \sum_{i \in U} \nabla \ell(\mathbf{w}_{E,B}; z_i), \mathbf{H}_{\text{NS}} = \frac{1}{n-m} \left(\sum_{i=1}^n \nabla^2 \ell(\mathbf{w}_{E,B}; z_i) - \sum_{i \in U} \nabla^2 \ell(\mathbf{w}_{E,B}; z_i) \right). \quad (15)$$

Infinitesimal Jackknife (IJ). Suriyakumar et al. [3] extends the work of NS by employing proximal IJ, and the main difference lies in the strategy of pre-computing and storing the inverse Hessian \mathbf{H}_{IJ} . It enables forgetting by adding the approximator $\mathbf{a}_{\text{IJ}}^{-u}$ to the learned model $\mathbf{w}_{E,B}$.

$$\mathbf{a}_{\text{IJ}}^{-u} = \frac{1}{n} \mathbf{H}_{\text{IJ}}^{-1} \nabla \ell(\mathbf{w}_{E,B}; u), \mathbf{H}_{\text{IJ}} = \frac{1}{n} \sum_{i=1}^n \nabla^2 \ell(\mathbf{w}_{E,B}; z_i). \quad (16)$$

Comparison of Pre-Computation. First, for a single data point u , Algorithm 1 entails computing the HVP of the gradient vectors $\nabla \ell(\mathbf{w}_{e,b}; u)$ T times, which requires $\mathcal{O}(Td)$ running time. To compute the our proposed hessian-free (HF) approximators $\mathbf{a}_{\text{HF}}^{-u}$ for all n samples, the complexity of running time is $\mathcal{O}(nTd)$. Our proposed method is highly efficient when dealing with overparameterized deep models, especially when $d \gg n$. This is because computing the full Hessian for NS requires $\mathcal{O}(nd^2)$ running time, and computing and inverting the full Hessian $\mathbf{H}_{\text{IJ}}^{-1}$ for IJ requires $\mathcal{O}(d^3 + nd^2)$.

Comparison of Storage. Algorithm 1 involves storing a vector of model parameter size for n data, requiring the storage of $\mathcal{O}(nd)$. This is lower than the overhead introduced by storing matrices for NS and IJ, which is $\mathcal{O}(d^2)$, when the dataset size n is lower than the dimension d of model parameters².

Comparison of Unlearning Computation. When a forgetting request with m data to be forgotten arrives, Algorithm 1 utilizes precomputed and prestored approximators to achieve forgetting, requiring a simple vector addition that takes $\mathcal{O}(md)$ time. For NS, it requires computing and inverting a different Hessian that depends on the user requesting the deletion. This necessitates substantial computational overhead of $\mathcal{O}(d^3 + md^2 + md)$ each time a deletion request arrives. Although IJ reduces this to $\mathcal{O}(md^2 + md)$, it is still not as efficient compared to our method.

²It's noteworthy that in the realm of deep neural networks for most computer vision tasks, dataset size n usually falls short of the model parameter dimension d . Even for neural language models, the empirical data-to-parameter scaling law is expected to remain at $n \sim d^{0.74}$, as suggested in [31].

5 Experiments

We devised the following experimental components: *verification and application*. Verification experiments are centered on evaluating the disparity between the unlearned and retrained models, across both convex and non-convex settings. Application experiments are geared towards evaluating the performance of different unlearning algorithms with a specific focus on determining the performance, pre-computation/storage, and unlearning time of these methods. Considering the space limit, we present a portion of the results from the verification experiments and application experiments, while deferring the remaining experiments to the [Appendix C](#).

5.1 Verification Experiments

Our principal aim is to validate the differences between the proposed Hessian-free (HF) approximator $\mathbf{a}_{\text{HF}}^{-U}$ and the actual $\mathbf{w}_{E,B}^{-U} - \mathbf{w}_{E,B}$, where a smaller difference indicates the unlearned model is closer to retrained model and also reflects the degree of data forgetting. Therefore, we evaluate the degree of forgetting from two perspectives: *distance and correlation*. Specifically, we use the L_2 norm $\|\mathbf{w}_{E,B}^{-U} - \mathbf{w}_{E,B} - \mathbf{a}^{-U}\|$ to measure the distance metric. A smaller distance metric indicates the approximators accurately capture the disparity between the retrained and learned models. Additionally, we utilize the Pearson [32] and Spearman [33] coefficient to assess the correlation between \mathbf{a}^{-U} and $\mathbf{w}_{E,B}^{-U} - \mathbf{w}_{E,B}$ by mapping them from high-dimensional space to scalar loss values, i.e. the approximate loss change $\ell(\mathbf{w}_{E,B} + \mathbf{a}^{-U}; U) - \ell(\mathbf{w}_{E,B}; U)$ and the actual loss change $\ell(\mathbf{w}_{E,B}^{-U}; U) - \ell(\mathbf{w}_{E,B}; U)$ on the forgetting dataset U . The resulting correlation scores range from -1 to 1, where the higher the correlation score, the more the unlearned model performs like the retrained model.

Configurations: We conduct experiments in both convex and non-convex scenarios. Specifically, we trained a multinomial Logistic Regression (LR) with total parameters $d = 7850$ and a simple convolutional neural network (CNN) with total parameters $d = 21840$ trained on MNIST [34] for handwriting digit classification. We apply a cross-entropy loss function and the inclusion of an L_2 regularization coefficient of 10^{-6} to ensure that the loss function of LR is strongly convex. For LR, training was performed for 100 epochs with stepsize of 0.05 and full batch. For CNN, training was carried out for 20 epochs with stepsize of 0.05 and a batch size of 64. Given these configurations mentioned above, we separately assessed the distance and correlation between our approximators $\mathbf{a}_{\text{HF}}^{-U}$, $\mathbf{a}_{\text{NS}}^{-U}$, $\mathbf{a}_{\text{IJ}}^{-U}$ at deletion rates in the set $\{1\%, 5\%, 10\%, 15\%, 20\%, 25\%, 30\%\}$. Following the suggestion in [35], a damping factor of 0.01 is added to the Hessian to ensure its invertibility when implementing NS and IJ. Besides, we conducted experiments with 7 random seeds to obtain average results. For the sake of clear visualizations, we use the minimum and maximum values as error bars.

The convex setting. As shown in [Figure 1](#) (a), our approach outperforms previous works. First, by distance evaluation, the approximation error $\|\Delta_{E,B}^{-U}\|$ of the proposed method is lower than that of the previous NS and IJ works. At a deletion rate of 30%, the approximation error is 0.171638, slightly lower than that of IJ and NS, which have errors of 0.178244 and 0.178246, respectively. Second, in assessing the loss change for the forgotten dataset U , our proposed method more accurately captures the changes in actual $\ell(\mathbf{w}_{E,B}^{-U}; U) - \ell(\mathbf{w}_{E,B}; U)$. In particular, when removing 30% of the samples, the proposed method maintains a high correlation, with Pearson and Spearman being 0.96 and 0.95, respectively. These evaluations demonstrate the efficacy of both Hessian-free and Hessian-based methods in accurately approximating the retrained model within convex settings. Our proposed approach not only achieves a closer approximation to the retrained model but also exhibits lower complexity compared to previous methods. This is substantiated by the results of Application Experiments I, which provide empirical evidence supporting our theoretical findings.

The non-convex setting. As illustrated in [Figure 1](#) (b), proposed HF method demonstrates superior performance, exhibiting less dependency on random variations compared to NS and IJ. When 30% of the samples are removed, our method maintains a lower approximation error of 0.96, surpassing the performance of IJ and NS. Our methods achieve Spearman and Pearson correlation coefficient of 0.80 and 0.74, respectively, accurately capturing actual loss changes, in contrast to IJ and NS which are far from the actual values in non-convex settings. In [Appendix C.1](#), we explain the volatility of the results in the prior works on non-convex setting, and provide more large-scale results, which is not achievable in NS and IJ [2, 3, 4] for their high complexity requirements and restrictive assumptions.

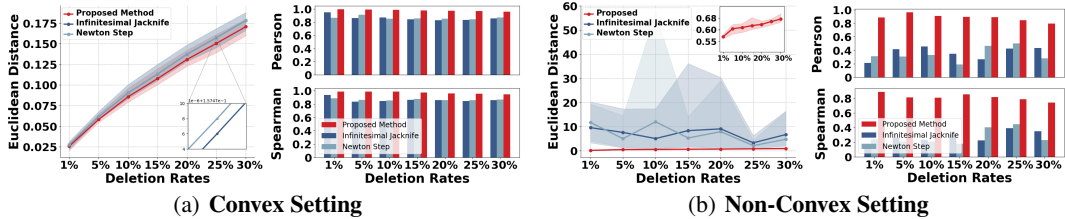


Figure 1: **Verification experiments I** on (a) LR and (b) CNN, respectively. The left of (a)(b) shows the distance to the retrained model, i.e. $\|\mathbf{w}_{E,B}^{-U} - \mathbf{w}_{E,B} - \mathbf{a}^{-U}\|$. The right of (a)(b) shows the correlation between the approximate and actual loss change on the forgetting data.

Table 2: **Application experiments I**. An online scenario with 20% data to be forgotten, where each unlearning request involves forgetting a single data point with each execution. The values in parenthesis represent the difference in test accuracy compared to the retrained model. We compute the total computational/storage cost for all samples and test the accuracy of the final unlearned model.

	Model	Unlearning Runtime (Sec)	Computation Speedup	PreComputation Runtime (Sec)	Storage (GB)	Test Accuracy (%) Unlearned model
NS	Logistic	5.14×10^2	$2.39 \times$	2.57×10^3	0.23	87.50 (-0.75)
	CNN	5.82×10^3	$0.05 \times$	2.91×10^4	1.78	83.50 (-10.25)
IJ	Logistic	1.84×10^0	$665 \times$	2.57×10^3	0.25	87.50 (-0.75)
	CNN	6.81×10^0	$45 \times$	2.91×10^4	1.78	82.75 (-11.00)
HF	Logistic	2.74×10^{-3}	$448,060 \times$	1.95×10^1	0.03	87.75 (-0.50)
	CNN	3.23×10^{-2}	$9,940 \times$	5.34×10^2	0.08	91.50 (-2.25)

5.2 Application Experiments

Furthermore, we compare the cost and performance of our method with the previous certified unlearning methods. Our evaluations are conducted from two perspectives: *runtime and utility*. Specifically, run-time focuses on the time spent precomputing unlearning statistics and the speedup of the unlearning algorithm compared to the retraining algorithm. Moreover, we evaluate the utility by the test accuracy of the unlearned model to ensure that generalization performance is not compromised. We train LR and simple CNN on MNIST with 20% data to be forgotten, which is identical to the aforementioned verification experiments I.

Application experiment results. Table 2 demonstrates that the proposed algorithm outperforms other baselines by a significant margin. Strikingly, the proposed algorithm outperforms benchmarks of certified unlearning regarding all metrics with millisecond-level unlearning and minimal performance degradation in both convex and non-convex settings. This demonstrates that the Hessian-free perspective method exhibits great potential for over-parameterized models compared to previous Hessian-based approaches. In Appendix C.2, we provide larger scale results, which is not achievable in previous work [2, 3, 4] due to their high complexity requirements and the restrictive assumptions.

6 Conclusion

In this work, we proposed a novel Hessian-free certified unlearning method. Specifically, we introduced an approximator based on affine stochastic recursion to characterize the trajectory discrepancy between the learned and retrained models. Our analysis does not involve inverting Hessian and thus can be extended to non-convex non-smooth objectives. Additionally, we provide theoretical results of generalization, unlearning guarantees, deletion capacity, and computation/storage complexity that are superior to state-of-the-art methods. Based on this analysis, we developed a certified unlearning algorithm that can achieve low-complexity and near-instantaneous unlearning. We employ HVP and gradient clipping techniques to mitigate the computation time and bound approximation error, respectively. We showed that proposed method can reduce the precomputation time, storage, and unlearning time (per sample) to $\mathcal{O}(nd)$, $\mathcal{O}(nd)$, $\mathcal{O}(d)$, respectively. Experimental results validate that our work benefits certified unlearning with reduced computation/storage and improved accuracy.

References

- [1] Chuan Guo, Tom Goldstein, Awni Y. Hannun, and Laurens van der Maaten. Certified data removal from machine learning models. In *Proceedings of the 37th International Conference on Machine Learning, ICML 2020, 13-18 July 2020, Virtual Event*, volume 119 of *Proceedings of Machine Learning Research*, pages 3832–3842. PMLR, 2020.
- [2] Ayush Sekhari, Jayadev Acharya, Gautam Kamath, and Ananda Theertha Suresh. Remember what you want to forget: Algorithms for machine unlearning. In *Advances in Neural Information Processing Systems 34, NeurIPS*, pages 18075–18086, 2021.
- [3] Vinith M. Suriyakumar, Ashia C. Wilson, et al. Algorithms that approximate data removal: New results and limitations. In *Advances in Neural Information Processing Systems 35, NeurIPS*, 2022.
- [4] Jiaqi Liu, Jian Lou, Zhan Qin, and Kui Ren. Certified minimax unlearning with generalization rates and deletion capacity. In *Advances in Neural Information Processing Systems 36: Annual Conference on Neural Information Processing Systems 2023, NeurIPS 2023.*, 2023.
- [5] Ananth Mahadevan and Michael Mathioudakis. Certifiable machine unlearning for linear models. *CoRR*, abs/2106.15093, 2021.
- [6] Eli Chien, Chao Pan, and Olgica Milenkovic. Efficient model updates for approximate unlearning of graph-structured data. In *The Eleventh International Conference on Learning Representations*, 2022.
- [7] Barak A. Pearlmutter. Fast exact multiplication by the hessian. *Neural Comput.*, 6(1):147–160, 1994.
- [8] Yinzhi Cao and Junfeng Yang. Towards making systems forget with machine unlearning. In *2015 IEEE Symposium on Security and Privacy, SP 2015, San Jose, CA, USA, May 17-21, 2015*, pages 463–480. IEEE Computer Society, 2015.
- [9] Lucas Bourtole, Varun Chandrasekaran, Christopher A. Choquette-Choo, Hengrui Jia, Adelin Travers, Baiwu Zhang, David Lie, and Nicolas Papernot. Machine unlearning. In *42nd IEEE Symposium on Security and Privacy, SP 2021, San Francisco, CA, USA, 24-27 May 2021*, pages 141–159. IEEE, 2021.
- [10] Jonathan Brophy and Daniel Lowd. Machine unlearning for random forests. In Marina Meila and Tong Zhang, editors, *Proceedings of the 38th International Conference on Machine Learning, ICML 2021, 18-24 July 2021, Virtual Event*, volume 139 of *Proceedings of Machine Learning Research*, pages 1092–1104. PMLR, 2021.
- [11] Sebastian Schelter, Stefan Grafberger, and Ted Dunning. Hedgecut: Maintaining randomised trees for low-latency machine unlearning. In Guoliang Li, Zhanhuai Li, Stratos Idreos, and Divesh Srivastava, editors, *SIGMOD '21: International Conference on Management of Data, Virtual Event, China, June 20-25, 2021*, pages 1545–1557. ACM, 2021.
- [12] Haonan Yan, Xiaoguang Li, Ziyao Guo, Hui Li, Fenghua Li, and Xiaodong Lin. ARCANE: an efficient architecture for exact machine unlearning. In *Proceedings of the Thirty-First International Joint Conference on Artificial Intelligence, IJCAI 2022, Vienna, Austria, 23-29 July 2022*, pages 4006–4013, 2022.
- [13] Min Chen, Zhikun Zhang, Tianhao Wang, Michael Backes, Mathias Humbert, and Yang Zhang. Graph unlearning. In Heng Yin, Angelos Stavrou, Cas Cremers, and Elaine Shi, editors, *Proceedings of the 2022 ACM SIGSAC Conference on Computer and Communications Security, CCS 2022, Los Angeles, CA, USA, November 7-11, 2022*, pages 499–513. ACM, 2022.
- [14] Chong Chen, Fei Sun, Min Zhang, and Bolin Ding. Recommendation unlearning. In Frédérique Laforest, Raphaël Troncy, Elena Simperl, Deepak Agarwal, Aristides Gionis, Ivan Herman, and Lionel Médini, editors, *WWW '22: The ACM Web Conference 2022, Virtual Event, Lyon, France, April 25 - 29, 2022*, pages 2768–2777. ACM, 2022.

- [15] Yinjun Wu, Edgar Dobriban, and Susan B. Davidson. Deltagrad: Rapid retraining of machine learning models. In *Proceedings of the 37th International Conference on Machine Learning, ICML 2020, 13-18 July 2020, Virtual Event*, volume 119 of *Proceedings of Machine Learning Research*, pages 10355–10366. PMLR, 2020.
- [16] Quoc Phong Nguyen, Bryan Kian Hsiang Low, and Patrick Jaillet. Variational bayesian unlearning. In Hugo Larochelle, Marc’Aurelio Ranzato, Raia Hadsell, Maria-Florina Balcan, and Hsuan-Tien Lin, editors, *Advances in Neural Information Processing Systems 33: Annual Conference on Neural Information Processing Systems 2020, NeurIPS 2020, December 6-12, 2020, virtual*, 2020.
- [17] Aditya Golatkar, Alessandro Achille, and Stefano Soatto. Eternal sunshine of the spotless net: Selective forgetting in deep networks. In *2020 IEEE/CVF Conference on Computer Vision and Pattern Recognition, CVPR 2020, Seattle, WA, USA, June 13-19, 2020*, pages 9301–9309. Computer Vision Foundation / IEEE, 2020.
- [18] Zachary Izzo, Mary Anne Smart, Kamalika Chaudhuri, and James Zou. Approximate data deletion from machine learning models. In *Proceedings of The 24th International Conference on Artificial Intelligence and Statistics*, pages 2008–2016, 2021.
- [19] Ronak Mehta, Sourav Pal, Vikas Singh, and Sathya N. Ravi. Deep unlearning via randomized conditionally independent Hessians. In *IEEE/CVF Conference on Computer Vision and Pattern Recognition, CVPR 2022, New Orleans, LA, USA, June 18-24, 2022*, pages 10412–10421. IEEE, 2022.
- [20] Ga Wu, Masoud Hashemi, and Christopher Srinivasa. PUMA: performance unchanged model augmentation for training data removal. In *Thirty-Sixth AAAI Conference on Artificial Intelligence, AAAI 2022, Thirty-Fourth Conference on Innovative Applications of Artificial Intelligence, IAAI 2022, The Twelveth Symposium on Educational Advances in Artificial Intelligence, EAAI 2022 Virtual Event, February 22 - March 1, 2022*, pages 8675–8682. AAAI Press, 2022.
- [21] Ryutaro Tanno, Melanie F. Pradier, Aditya V. Nori, and Yingzhen Li. Repairing neural networks by leaving the right past behind. In *NeurIPS*, 2022.
- [22] Alexander Becker and Thomas Liebig. Certified data removal in sum-product networks. In Peipei Li, Kui Yu, Nitesh V. Chawla, Ronen Feldman, Qing Li, and Xindong Wu, editors, *IEEE International Conference on Knowledge Graph, ICKG 2022, Orlando, FL, USA, November 30 - Dec. 1, 2022*, pages 14–21. IEEE, 2022.
- [23] Matthew Jagielski, Om Thakkar, Florian Tramèr, Daphne Ippolito, Katherine Lee, Nicholas Carlini, Eric Wallace, Shuang Song, Abhradeep Guha Thakurta, Nicolas Papernot, and Chiyuan Zhang. Measuring forgetting of memorized training examples. In *The Eleventh International Conference on Learning Representations, ICLR 2023, Kigali, Rwanda, May 1-5, 2023*. OpenReview.net, 2023.
- [24] Alexander Warnecke, Lukas Pirch, Christian Wressnegger, and Konrad Rieck. Machine unlearning of features and labels. In *30th Annual Network and Distributed System Security Symposium, NDSS 2023, San Diego, California, USA, February 27 - March 3, 2023*. The Internet Society, 2023.
- [25] Ayush Kumar Tarun, Vikram Singh Chundawat, Murari Mandal, and Mohan S. Kankanhalli. Deep regression unlearning. In Andreas Krause, Emma Brunskill, Kyunghyun Cho, Barbara Engelhardt, Sivan Sabato, and Jonathan Scarlett, editors, *International Conference on Machine Learning, ICML 2023, 23-29 July 2023, Honolulu, Hawaii, USA*, volume 202 of *Proceedings of Machine Learning Research*, pages 33921–33939. PMLR, 2023.
- [26] Varun Gupta, Christopher Jung, Seth Neel, Aaron Roth, Saeed Sharifi-Malvajerdi, and Chris Waites. Adaptive machine unlearning. In Marc’Aurelio Ranzato, Alina Beygelzimer, Yann N. Dauphin, Percy Liang, and Jennifer Wortman Vaughan, editors, *Advances in Neural Information Processing Systems 34: Annual Conference on Neural Information Processing Systems 2021, NeurIPS 2021, December 6-14, 2021, virtual*, pages 16319–16330, 2021.

- [27] Seth Neel, Aaron Roth, and Saeed Sharifi-Malvajerdi. Descent-to-delete: Gradient-based methods for machine unlearning. In Vitaly Feldman, Katrina Ligett, and Sivan Sabato, editors, *Algorithmic Learning Theory, 16-19 March 2021, Virtual Conference, Worldwide*, volume 132 of *Proceedings of Machine Learning Research*, pages 931–962. PMLR, 2021.
- [28] Priya Goyal, Piotr Dollár, Ross B. Girshick, Pieter Noordhuis, Lukasz Wesolowski, Aapo Kyrola, Andrew Tulloch, Yangqing Jia, and Kaiming He. Accurate, large minibatch SGD: training imagenet in 1 hour. *CoRR*, abs/1706.02677, 2017.
- [29] Mert Gürbüzbalaban, Umut Simsekli, and Lingjiong Zhu. The heavy-tail phenomenon in SGD. In Marina Meila and Tong Zhang, editors, *Proceedings of the 38th International Conference on Machine Learning, ICML 2021, 18-24 July 2021, Virtual Event*, volume 139 of *Proceedings of Machine Learning Research*, pages 3964–3975. PMLR, 2021.
- [30] Jingzhao Zhang, Tianxing He, Suvrit Sra, and Ali Jadbabaie. Why gradient clipping accelerates training: A theoretical justification for adaptivity. In *8th International Conference on Learning Representations, ICLR 2020, Addis Ababa, Ethiopia, April 26-30, 2020*, 2020.
- [31] Jared Kaplan, Sam McCandlish, Tom Henighan, Tom B. Brown, Benjamin Chess, Rewon Child, Scott Gray, Alec Radford, Jeffrey Wu, and Dario Amodei. Scaling laws for neural language models. *CoRR*, abs/2001.08361, 2020.
- [32] Sewall Wright. Correlation and causation. *Journal of agricultural research*, 20(7):557–585, 1921.
- [33] Charles Spearman. The proof and measurement of association between two things. 1961.
- [34] Li Deng. The mnist database of handwritten digit images for machine learning research. *IEEE Signal Processing Magazine*, 29(6):141–142, 2012.
- [35] Samyadeep Basu, Phillip Pope, and Soheil Feizi. Influence functions in deep learning are fragile. In *9th International Conference on Learning Representations, ICLR 2021, Virtual Event, Austria, May 3-7, 2021*. OpenReview.net, 2021.
- [36] Ningxin Su and Baochun Li. Asynchronous federated unlearning. In *IEEE INFOCOM 2023 - IEEE Conference on Computer Communications, New York City, NY, USA, May 17-20, 2023*, pages 1–10. IEEE, 2023.
- [37] Antonio Ginart, Melody Guan, Gregory Valiant, and James Y Zou. Making ai forget you: Data deletion in machine learning. *Advances in neural information processing systems*, 32, 2019.
- [38] Korbinian Koch and Marcus Soll. No matter how you slice it: Machine unlearning with sisa comes at the expense of minority classes. In *2023 IEEE Conference on Secure and Trustworthy Machine Learning (SaTML)*, pages 622–637. IEEE, 2023.
- [39] Meghdad Kurmanji, Peter Triantafillou, Jamie Hayes, and Eleni Triantafillou. Towards unbounded machine unlearning. *Advances in Neural Information Processing Systems*, 36, 2024.
- [40] Anisa Halimi, Swanand Kadhe, Ambrish Rawat, and Nathalie Baracaldo. Federated unlearning: How to efficiently erase a client in fl? *arXiv preprint arXiv:2207.05521*, 2022.
- [41] Pang Wei Koh and Percy Liang. Understanding black-box predictions via influence functions. In Doina Precup and Yee Whye Teh, editors, *Proceedings of the 34th International Conference on Machine Learning, ICML 2017, Sydney, NSW, Australia, 6-11 August 2017*, volume 70 of *Proceedings of Machine Learning Research*, pages 1885–1894. PMLR, 2017.
- [42] Samyadeep Basu, Xuchen You, and Soheil Feizi. On second-order group influence functions for black-box predictions. In *Proceedings of the 37th International Conference on Machine Learning, ICML 2020, 13-18 July 2020, Virtual Event*, volume 119 of *Proceedings of Machine Learning Research*, pages 715–724. PMLR, 2020.
- [43] Cynthia Dwork. Differential privacy. In *International colloquium on automata, languages, and programming*, pages 1–12. Springer, 2006.

- [44] Aditya Golatkar, Alessandro Achille, and Stefano Soatto. Forgetting outside the box: Scrubbing deep networks of information accessible from input-output observations. In Andrea Vedaldi, Horst Bischof, Thomas Brox, and Jan-Michael Frahm, editors, *Computer Vision - ECCV 2020 - 16th European Conference, Glasgow, UK, August 23-28, 2020, Proceedings, Part XXIX*, volume 12374 of *Lecture Notes in Computer Science*, pages 383–398. Springer, 2020.
- [45] Aditya Golatkar, Alessandro Achille, Avinash Ravichandran, Marzia Polito, and Stefano Soatto. Mixed-privacy forgetting in deep networks. In *IEEE Conference on Computer Vision and Pattern Recognition, CVPR 2021, virtual, June 19-25, 2021*, pages 792–801. Computer Vision Foundation / IEEE, 2021.
- [46] Shai Shalev-Shwartz, Ohad Shamir, Nathan Srebro, and Karthik Sridharan. Stochastic convex optimization. In *COLT 2009 - The 22nd Conference on Learning Theory, Montreal, Quebec, Canada, June 18-21, 2009*, 2009.
- [47] Kaiming He, Xiangyu Zhang, Shaoqing Ren, and Jian Sun. Deep residual learning for image recognition. In *2016 IEEE Conference on Computer Vision and Pattern Recognition, CVPR 2016, Las Vegas, NV, USA, June 27-30, 2016*, pages 770–778. IEEE Computer Society, 2016.
- [48] Krizhevsky Alex. Learning multiple layers of features from tiny images. <https://www.cs.toronto.edu/kriz/learning-features-2009-TR.pdf>, 2009.
- [49] Ziwei Liu, Ping Luo, Xiaogang Wang, and Xiaoou Tang. Deep learning face attributes in the wild. In *Proceedings of International Conference on Computer Vision (ICCV)*, December 2015.
- [50] Gary B. Huang, Manu Ramesh, Tamara Berg, and Erik Learned-Miller. Labeled faces in the wild: A database for studying face recognition in unconstrained environments. Technical Report 07-49, University of Massachusetts, Amherst, October 2007.
- [51] Lei Wu, Chao Ma, and Weinan E. How SGD selects the global minima in over-parameterized learning: A dynamical stability perspective. In Samy Bengio, Hanna M. Wallach, Hugo Larochelle, Kristen Grauman, Nicolò Cesa-Bianchi, and Roman Garnett, editors, *Advances in Neural Information Processing Systems 31: Annual Conference on Neural Information Processing Systems 2018, NeurIPS 2018, December 3-8, 2018, Montréal, Canada*, pages 8289–8298, 2018.
- [52] Justin Gilmer, Behrooz Ghorbani, Ankush Garg, Sneha Kudugunta, Behnam Neyshabur, David Cardoze, George Edward Dahl, Zachary Nado, and Orhan Firat. A loss curvature perspective on training instabilities of deep learning models. In *International Conference on Learning Representations*, 2022.
- [53] Levent Sagun, Utku Evci, V. Ugur Güney, Yann N. Dauphin, and Léon Bottou. Empirical analysis of the hessian of over-parametrized neural networks. In *6th International Conference on Learning Representations, ICLR 2018, Vancouver, BC, Canada, April 30 - May 3, 2018, Workshop Track Proceedings*. OpenReview.net, 2018.
- [54] Levent Sagun, Leon Bottou, and Yann LeCun. Eigenvalues of the hessian in deep learning: Singularity and beyond. *arXiv preprint arXiv:1611.07476*, 2016.
- [55] Kaiyue Wen, Tengyu Ma, and Zhiyuan Li. How sharpness-aware minimization minimizes sharpness? In *The Eleventh International Conference on Learning Representations, ICLR 2023, Kigali, Rwanda, May 1-5, 2023*. OpenReview.net, 2023.
- [56] Pierre Foret, Ariel Kleiner, Hossein Mobahi, and Behnam Neyshabur. Sharpness-aware minimization for efficiently improving generalization. In *9th International Conference on Learning Representations, ICLR 2021, Virtual Event, Austria, May 3-7, 2021*. OpenReview.net, 2021.

A An Expanded Version of The Related Work

Machine Unlearning, the terminology can be traced back to the paper of Cao et al. [8], and their work defined the notion of "the completeness of forgetting". There are two main categories based on the completeness of forgetting: Exact Unlearning and Approximate Unlearning.

Exact Unlearning aims to accelerate the speed of retraining and completely eliminate the influence of forgotten data on learned model. The majority of existing Exact Unlearning methods are derived from the work of Bourtole et al. [9], which proposed the notable SISA framework, grounded in ensemble learning techniques. Specifically, the training dataset is partitioned into mutually disjoint shards, and then sub-models are trained on these shards. Upon unlearning, SISA only needs to retrain the sub-model correlated with the relevant data shard and then make the final prediction by assembling the knowledge of each sub-model, which significantly lowers retraining computational costs. Under the SISA framework, other Exact Unlearning methods have also been proposed, e.g., GraphEraser [13] extended SISA to graph learning by partitioning the original training graph into disjoint shards, parallelly training a set of shard models, and learning an optimal importance score for each shard model. RecEraser [14] extended SISA to recommendation systems. KNOT [36] adopted the SISA for client-level asynchronous federated unlearning during training and introduced a clustered mechanism that divides clients into multiple clusters. Other methods, such as DaRE [10] and HedgeCut [11], addressed the issue that SISA cannot be applied to decision trees and proposed exact unlearning solutions; and [37] aimed to achieve forgetting in K-means clustering. Furthermore, ARCANE [12] introduced a class-based data partitioning strategy that enhances the performance of SISA.

However, the SISA framework adopts a structure that completely separates the data, resembling ensemble learning approaches where predictions or models are aggregated only at the end. This separation restricts the model training process from fully leveraging the entirety of the segmented datasets and also hampers its extensibility, consequently leading to lower accuracy and performance compared to a model trained on the entire unsegmented dataset. In an experimental evaluation conducted by Koch et al. [38], it was found that simply down-sampling the dataset to achieve a more balanced single shard outperforms SISA in terms of both unlearning speed and performance.

Approximate Unlearning thus seeks to minimize the impact of forgetting data to an acceptable level to trade off for computational efficiency, reduced storage costs, and flexibility. There are many approaches to realizing Approximate Unlearning, such as [39] developed a distillation-based method; [40] adopted a gradient ascent approach on the forgotten data to achieve forgetting. Among these, second-order methods have been widely studied, with most of these methods (e.g., [2, 3, 4, 6, 26, 27]) inspired by influence function studies [41, 35, 42], aiming to extract information from the Hessian of the loss function and achieve forgetting through limited model updates. In particular, inspired by differential privacy [43], Guo et al. [1] introduced a (ϵ, δ) -certified unlearning definition, anticipating ensuring the output distribution of the unlearning algorithm is indistinguishable from that of retraining. Furthermore, due to the high computational cost of the Hessian, Fisher-based methods [17, 44, 45] have emerged to approximate the Hessian. Our paper focuses on Hessian-based certified unlearning.

Among these Hessian-based certified unlearning methods, Sekhari et al. [2]; Suriyakumar et al. [3]; Liu et al. [4] established the theoretical foundation for Hessian-based methods and provided the generalization result in terms of the population risk, as well as derived the deletion capacity guarantee. In the definition of certified unlearning, [2, 3, 4] align with our method, which lies in pre-computing statistics of data that extract second-order information from the Hessian and using these 'recollections' to forget data. In particular, Sekhari et al. [2] pointed out the importance of providing the generalization performance after machine unlearning and proposed achieving forgetting upon the arrival of a forgetting request using a Newton step through the precomputation and storage of the Hessian offline. Suriyakumar et al. [3, 4] extended the work of Sekhari et al. [2], attaining strong convexity through a non-smooth regularizer by leveraging the proximal IJ. Moreover, by trading off the offline computation time to invert the Hessian, the unlearning time was reduced to $\mathcal{O}(d^2)$. Liu et al. [4] further developed an (ϵ, δ) -certified unlearning algorithm for minimax models.

However, these second-order certified unlearning methods have encountered persistent challenges that are difficult to overcome. That is, existing certified unlearning methods, especially those focused on establishing theoretical results, have largely focused on strongly convex and smooth objectives. Moreover, prior second-order methods require expensive Hessian computations, thus suffering from the curse of model parameter dimensionality, making it challenging to apply to most deep model.

B Proofs

B.1 Detailed Analysis of Equation (10)

Here, we provide a more detailed proof and explanation for (10). Specifically, we first consider the impact of sample u during the e -th epoch, and then extend the analysis to all epochs.

It should be noted that a necessary setting for our method is that the retraining and learning process have the same initialization, model architecture, and training process.

Analysis of (10). Since each sample participates in updates only once per epoch, without loss of generality, for the e -th epoch, we define the sample u to be involved (sampled) in the $b(u)$ -th update of the e -th epoch. Therefore, for a learning model in (3) and a retraining model obtained without the knowledge of u in (4), we have that the following one step updates,

$$\begin{aligned}\mathbf{w}_{e,b+1}^{-u} &\leftarrow \mathbf{w}_{e,b}^{-u} - \frac{\eta_{e,b}}{|\mathcal{B}_{e,b}|} \sum_{i \in \mathcal{B}_{e,b}} \nabla \ell(\mathbf{w}_{e,b}^{-u}; z_i), \\ \mathbf{w}_{e,b+1} &\leftarrow \mathbf{w}_{e,b} - \frac{\eta_{e,b}}{|\mathcal{B}_{e,b}|} \sum_{i \in \mathcal{B}_{e,b}} \nabla \ell(\mathbf{w}_{e,b}; z_i).\end{aligned}\tag{17}$$

When the update includes sample u during e -th epoch's $b(u)$ -th update, consider the linear scaling rule proposed in [28], i.e., the retraining stepsize $\hat{\eta}_{e,b(u)} = \eta_{e,b(u)} \frac{|\mathcal{B}_{e,b(u)} \setminus \{u\}|}{|\mathcal{B}_{e,b(u)}|}$, we have,

$$\begin{aligned}\mathbf{w}_{e,b(u)+1}^{-u} &\leftarrow \mathbf{w}_{e,b(u)}^{-u} - \frac{\eta_{e,b(u)}}{|\mathcal{B}_{e,b(u)}|} \sum_{i \in \mathcal{B}_{e,b(u)} \setminus \{u\}} \nabla \ell(\mathbf{w}_{e,b(u)}^{-u}; z_i), \\ \mathbf{w}_{e,b(u)+1} &\leftarrow \mathbf{w}_{e,b(u)} - \frac{\eta_{e,b(u)}}{|\mathcal{B}_{e,b(u)}|} \sum_{i \in \mathcal{B}_{e,b(u)}} \nabla \ell(\mathbf{w}_{e,b(u)}; z_i).\end{aligned}\tag{18}$$

Consider the Taylor expansion of $\nabla \ell(\mathbf{w}_{e,b}^{-u}; z_i)$ around $\mathbf{w}_{e,b}$, we have,

$$\nabla \ell(\mathbf{w}_{e,b}^{-u}; z_i) = \nabla \ell(\mathbf{w}_{e,b}; z_i) + \nabla^2 \ell(\mathbf{w}_{e,b}; z_i)(\mathbf{w}_{e,b}^{-u} - \mathbf{w}_{e,b}) + o(\mathbf{w}_{e,b}^{-u} - \mathbf{w}_{e,b}),\tag{19}$$

where $\mathbf{H}_{e,b} = \sum_{i \in \mathcal{B}_{e,b}} \nabla^2 \ell(\mathbf{w}_{e,b}; z_i)$ denote the Hessian of the loss during the e -th epoch's b -th update. Therefore, for (17) and (18), we can approximate the SGD recursion as,

$$\begin{aligned}\mathbf{w}_{e,b+1}^{-u} - \mathbf{w}_{e,b+1} &\approx (\mathbf{I} - \frac{\eta_{e,b}}{|\mathcal{B}_{e,b}|} \mathbf{H}_{e,b})(\mathbf{w}_{e,b}^{-u} - \mathbf{w}_{e,b}), \\ \mathbf{w}_{e,b(u)+1}^{-u} - \mathbf{w}_{e,b(u)+1} &\approx \underbrace{(\mathbf{I} - \frac{\eta_{e,b(u)}}{|\mathcal{B}_{e,b(u)}|} \mathbf{H}_{e,b(u)})(\mathbf{w}_{e,b(u)}^{-u} - \mathbf{w}_{e,b(u)})}_{\text{Approximate impact of } u \text{ in previous epochs}} + \underbrace{\frac{\eta_{e,b(u)}}{|\mathcal{B}_{e,b(u)}|} \nabla \ell(\mathbf{w}_{e,b(u)}; u)}_{\text{Approximate impact of } u \text{ in } e\text{-th epoch}}.\end{aligned}\tag{20}$$

Therefore, during the E -th epoch, the difference between the retraining model and the learning model is approximately as,

$$\begin{aligned}\mathbf{w}_{E,B}^{-u} - \mathbf{w}_{E,B} &\approx \prod_{b=0}^{B-1} (\mathbf{I} - \frac{\eta_{E,b}}{|\mathcal{B}_{E,b}|} \mathbf{H}_{E,b})(\mathbf{w}_{E,0}^{-u} - \mathbf{w}_{E,0}) \\ &\quad + \prod_{b=b(u)}^{B-1} (\mathbf{I} - \frac{\eta_{E,b}}{|\mathcal{B}_{E,b}|} \mathbf{H}_{E,b}) \frac{\eta_{E,b(u)}}{|\mathcal{B}_{E,b(u)}|} \nabla \ell(\mathbf{w}_{E,b(u)}; u).\end{aligned}\tag{21}$$

We have thus obtained the difference between the retraining model and the learning model in the E -th epoch. It is worth noting that the second term represents the influence of sample u on the training trajectory during the E -th epoch, and it can be computed entirely. In the first term, $\mathbf{w}_{E,0}^{-u} - \mathbf{w}_{E,0} = \mathbf{w}_{E-1,B}^{-u} - \mathbf{w}_{E-1,B}$ is the result of the $E-1$ -th epoch, and for the $E-1$ epoch, we also have a similar result. Since the initial models are identical, apply it recursively to complete the proof and, we ultimately obtain the approximator for u .

$$\mathbf{w}_{E,B}^{-u} - \mathbf{w}_{E,B} \approx \sum_{e=0}^E \mathbf{M}_{e,b(u)} \nabla \ell(\mathbf{w}_{e,b(u)}; u) := \mathbf{a}_{E,B}^{-u}.\tag{22}$$

where $\mathbf{M}_{e,b(u)} = \frac{\eta_{e,b(u)}}{|\mathcal{B}_{e,b(u)}|} \prod_{k=e}^E \prod_{b=b(u)+1}^{B-1} (\mathbf{I} - \frac{\eta_{k,b}}{|\mathcal{B}_{k,b}|} \mathbf{H}_{k,b})$. \square

B.2 Detailed Proof of Theorem 1

Now, we demonstrate that in the case of continuous arrival of deletion requests, our algorithm is capable of streaming removing samples. Intuitively, this property can be mainly explained by Taylor's linear expansion. For ease of exposition, we simplify our proof to a scenario with only two samples, u_1 and u_2 . That is, our goal is to prove that when u_1 initiates a deletion request and the algorithm is executed, the arrival of a deletion request from u_2 after u_1 (*Streaming Deletion*), is fully equivalent to the simultaneous execution of deletion requests from both u_1 and u_2 (*Batch Deletion*).

Without loss of generality, we assume that $b(u_1) < b(u_2)$. Based on (10), the approximators for u_1 and u_2 are denoted as $\mathbf{a}_{E,B}^{-u_1}$ and $\mathbf{a}_{E,B}^{-u_2}$, respectively, as follows:

$$\begin{aligned}\mathbf{a}_{E,B}^{-u_1} &= \sum_{e=0}^E \mathbf{M}_{e,b(u_1)} \nabla \ell(\mathbf{w}_{e,b(u_1)}; u_1), \\ \mathbf{a}_{E,B}^{-u_2} &= \sum_{e=0}^E \mathbf{M}_{e,b(u_2)} \nabla \ell(\mathbf{w}_{e,b(u_2)}; u_2).\end{aligned}\tag{23}$$

When we simultaneously delete u_1 and u_2 , the difference between retraining the model and learning the model is as follows,

$$\mathbf{w}_{e,b+1}^{-u_2-u_1} - \mathbf{w}_{e,b+1} \leftarrow \mathbf{w}_{e,b}^{-u_2-u_1} - \mathbf{w}_{e,b} - \frac{\eta_{e,b}}{|\mathcal{B}_{e,b}|} \sum_{i \in \mathcal{B}_{e,b}} \left(\nabla \ell(\mathbf{w}_{e,b}^{-u_2-u_1}; z_i) - \nabla \ell(\mathbf{w}_{e,b}; z_i) \right).\tag{24}$$

Consider the Taylor expansion during the E -th epoch, we have,

$$\mathbf{w}_{E,b+1}^{-u_2-u_1} - \mathbf{w}_{E,b+1} \approx \left(\mathbf{I} - \frac{\eta_{E,b}}{|\mathcal{B}_{E,b}|} \mathbf{H}_{E,b} \right) (\mathbf{w}_{E,b}^{-u_2-u_1} - \mathbf{w}_{E,b}).\tag{25}$$

When u_1 and u_2 are removed respectively, we have the following approximation:

$$\begin{aligned}\mathbf{w}_{E,b(u_2)+1}^{-u_2-u_1} - \mathbf{w}_{E,b(u_2)+1} &\approx \left(\mathbf{I} - \frac{\eta_{E,b(u_2)}}{|\mathcal{B}_{E,b(u_2)}|} \mathbf{H}_{E,b(u_2)} \right) (\mathbf{w}_{E,b(u_2)}^{-u_2-u_1} - \mathbf{w}_{E,b(u_2)}) \\ &\quad + \underbrace{\frac{\eta_{E,b(u_2)}}{|\mathcal{B}_{E,b(u_2)}|} \nabla \ell(\mathbf{w}_{E,b(u_2)}; u_2)}_{\text{Approximate impact of } u_2 \text{ in } e\text{-th epoch}}, \\ \mathbf{w}_{E,b(u_1)+1}^{-u_2-u_1} - \mathbf{w}_{E,b(u_1)+1} &\approx \left(\mathbf{I} - \frac{\eta_{E,b(u_1)}}{|\mathcal{B}_{E,b(u_1)}|} \mathbf{H}_{E,b(u_1)} \right) (\mathbf{w}_{E,b(u_1)}^{-u_2-u_1} - \mathbf{w}_{E,b(u_1)}) \\ &\quad + \underbrace{\frac{\eta_{E,b(u_2)}}{|\mathcal{B}_{E,b(u_2)}|} \nabla \ell(\mathbf{w}_{E,b(u_2)}; u_2)}_{\text{Approximate impact of } u_2 \text{ in } e\text{-th epoch}} + \underbrace{\frac{\eta_{E,b(u_1)}}{|\mathcal{B}_{E,b(u_1)}|} \nabla \ell(\mathbf{w}_{E,b(u_1)}; u_1)}_{\text{Approximate impact of } u_1 \text{ in } e\text{-th epoch}}.\end{aligned}\tag{26}$$

Therefore, in the E -th epoch, we have the following affine stochastic recursion,

$$\begin{aligned}\mathbf{w}_{E,B}^{-u_2-u_1} - \mathbf{w}_{E,B} &\approx \prod_{b=0}^{B-1} \left(\mathbf{I} - \frac{\eta_{E,b}}{|\mathcal{B}_{E,b}|} \mathbf{H}_{E,b} \right) (\mathbf{w}_{E,0}^{-u_2-u_1} - \mathbf{w}_{E,0}) \\ &\quad + \prod_{b=b(u_1)}^{B-1} \left(\mathbf{I} - \frac{\eta_{E,b}}{|\mathcal{B}_{E,b}|} \mathbf{H}_{E,b} \right) \frac{\eta_{E,b(u_1)}}{|\mathcal{B}_{E,b(u_1)}|} \nabla \ell(\mathbf{w}_{E,b(u_1)}; u_1) \\ &\quad + \prod_{b=b(u_2)}^{B-1} \left(\mathbf{I} - \frac{\eta_{E,b}}{|\mathcal{B}_{E,b}|} \mathbf{H}_{E,b} \right) \frac{\eta_{E,b(u_2)}}{|\mathcal{B}_{E,b(u_2)}|} \nabla \ell(\mathbf{w}_{E,b(u_2)}; u_2).\end{aligned}\tag{27}$$

Apply it recursively to complete the proof, and we can simultaneously compute the impact of u_1 and u_2 on training for all epochs. Since the initial models are identical, recursion stops at $e = 0, b = b(u_1)$, and we eventually obtain,

$$\mathbf{w}_{E,B}^{-u_2-u_1} - \mathbf{w}_{E,B} \approx \sum_{e=0}^E \mathbf{M}_{e,b(u_1)} \nabla \ell(\mathbf{w}_{e,b(u_1)}; u_1) + \sum_{e=0}^E \mathbf{M}_{e,b(u_2)} \nabla \ell(\mathbf{w}_{e,b(u_2)}; u_2) := \mathbf{a}_{E,B}^{-u_2-u_1}.\tag{28}$$

According to (23) and (28), we have completed the proof of $\mathbf{a}_{E,B}^{-u_2-u_1} = \mathbf{a}_{E,B}^{-u_1} + \mathbf{a}_{E,B}^{-u_2}$.

B.3 Detailed Proof of Lemma 2

Proof of Lemma 2. Now we begin the proof that the remainder term $o(\mathbf{w}_{e,b}^{-u} - \mathbf{w}_{e,b})$ in the e -th epoch, b -th round is bounded by gradient clipping. Specifically, recalling (4), we have,

$$\begin{aligned} \mathbf{w}_{e,b+1}^{-u} - \mathbf{w}_{e,b+1} &\approx \mathbf{w}_{e,b}^{-u} - \mathbf{w}_{e,b} - \frac{\eta_{e,b}}{|\mathcal{B}_{e,b}|} \sum_{i \in \mathcal{B}_{e,b}} \left(\nabla \ell(\mathbf{w}_{e,b}^{-u}; z_i) - \nabla \ell(\mathbf{w}_{e,b}; z_i) \right), \\ \mathbf{w}_{e,b(u)+1}^{-u} - \mathbf{w}_{e,b(u)+1} &\approx \mathbf{w}_{e,b(u)}^{-u} - \mathbf{w}_{e,b(u)} \\ &\quad - \frac{\eta_{e,b(u)}}{|\mathcal{B}_{e,b(u)}|} \sum_{i \in \mathcal{B}_{e,b(u)} \setminus \{u\}} \left(\nabla \ell(\mathbf{w}_{e,b(u)}^{-u}; z_i) - \nabla \ell(\mathbf{w}_{e,b(u)}; z_i) \right) + \frac{\eta_{e,b(u)}}{|\mathcal{B}_{e,b(u)}|} \nabla \ell(\mathbf{w}_{e,b(u)}; u). \end{aligned} \quad (29)$$

In model training, we threshold the stochastic gradient norm $\|\nabla \ell(\mathbf{w}_{e,b}; u)\|$ at C when clipping is applied.

$$\|\mathbf{w}_{e,b}^{-u} - \mathbf{w}_{e,b}\| \leq \|\mathbf{w}_{e,b-1}^{-u} - \mathbf{w}_{e,b-1}\| + 2\eta_{e,b-1}C. \quad (30)$$

Consider a simple stepsize time decay strategy $\eta_{e,b} = q\eta_{e,b-1}$, where $0 < q < 1$ is the decay rate, and let η be the initial stepsize. Recalling that $t = eB + b$, then we get

$$\|\mathbf{w}_{e,b}^{-u} - \mathbf{w}_{e,b}\| \leq \|\mathbf{w}_{e,b-1}^{-u} - \mathbf{w}_{e,b-1}\| + 2\eta C q^{t-1}. \quad (31)$$

Note that the initial retraining model and learning model are identical. Therefore, based on the above recursion, we can obtain the geometric progression as follows,

$$\begin{aligned} \|\mathbf{w}_{e,b}^{-u} - \mathbf{w}_{e,b}\| &\leq 2\eta C q^{t-1} + 2\eta C q^{t-2} + \dots + 2\eta C q^0 \\ &= 2\eta C \sum_{k=0}^{t-1} q^k \\ &= 2\eta C \frac{q^t - 1}{q - 1}. \end{aligned} \quad (32)$$

Therefore, we have completed the proof. \square

B.4 Detailed Proof of Theorem 4

Proof of Theorem 4. Let us recall the approximator of (10) in Section 3, we have,

$$\begin{aligned} \mathbf{a}_{E,B}^{-u} &= \sum_{e=1}^E \mathbf{M}_{e,b(u)} \nabla \ell(\mathbf{w}_{e,b(u)}; u), \\ \text{where } \mathbf{M}_{e,b(u)} &= \frac{\eta_{e,b(u)}}{|\mathcal{B}_{e,b(u)}|} \prod_{k=e}^E \prod_{b=b(u)+1}^{B-1} \left(\mathbf{I} - \frac{\eta_{k,b}}{|\mathcal{B}_{k,b}|} \mathbf{H}_{k,b} \right). \end{aligned} \quad (33)$$

For the E -th epoch' B -th update, we have the following Taylor approximation,

$$\begin{aligned} \mathbf{w}_{E,B}^{-u} - \mathbf{w}_{E,B} - \mathbf{a}_{E,B}^{-u} &= \left(\mathbf{I} - \frac{\eta_{E,B-1}}{|\mathcal{B}_{E,B-1}|} \mathbf{H}_{E,B-1} \right) (\mathbf{w}_{E,B-1}^{-u} - \mathbf{w}_{E,B-1}) \\ &\quad + \eta_{E,B-1} o(\mathbf{w}_{E,B-1}^{-u} - \mathbf{w}_{E,B-1}) - \mathbf{a}_{E,B}^{-u}. \end{aligned} \quad (34)$$

For convenience, we define $\Delta_{E,B}^{-u} = \mathbf{w}_{E,B}^{-u} - \mathbf{w}_{E,B}$, and $\hat{\mathbf{H}}_{E,B-1} = \mathbf{I} - \frac{\eta_{E,B-1}}{|\mathcal{B}_{E,B-1}|} \mathbf{H}_{E,B-1}$. Here, we begin to analyze the error generated by each update,

$$\Delta_{E,B}^{-u} - \mathbf{a}_{E,B}^{-u} = \hat{\mathbf{H}}_{E,B-1} \Delta_{E,B-1}^{-u} + \eta_{E,B-1} o(\Delta_{E,B-1}^{-u}) - \mathbf{a}_{E,B}^{-u}, \quad (35)$$

Furthermore, we observe that during the E -th epoch, (35) can be obtained from affine stochastic recursion as follows,

$$\begin{aligned}
\|\Delta_{E,B}^{-u} - \mathbf{a}_{E,B}^{-u}\| &\leq \left\| \prod_{b=0}^{B-1} \hat{\mathbf{H}}_{E,b} \Delta_{E,0}^{-u} - \mathbf{a}_{E-1,B}^{-u} \right\| \\
&\quad + \underbrace{\frac{\eta q^{T-B+b(u)}}{|\mathcal{B}_{E,b(u)}|} \left\| \prod_{b=b(u)+1}^{B-1} \hat{\mathbf{H}}_{E,b} \left(\nabla \ell(\mathbf{w}_{E,b(u)}^{-u}; u) - \nabla \ell(\mathbf{w}_{E,b(u)}; u) \right) \right\|}_{\text{Approximation error term } C_2 \text{ during the } E\text{-th epoch}} \\
&\quad + \underbrace{\eta q^{T-1} \|\Delta_{E,B-1}^{-u}\| + \eta q^{T-2} \|\hat{\mathbf{H}}_{E,B-1} \Delta_{E,B-2}^{-u}\| + \dots + \eta q^{T-B} \left\| \prod_{b=0}^{B-1} \hat{\mathbf{H}}_{E,b} \Delta_{E,0}^{-u} \right\|}_{\text{Approximation error term } C_1 \text{ during the } E\text{-th epoch}}.
\end{aligned} \tag{36}$$

Through the above process, we obtain the result of the E -th epoch approximation. Now let's bound the last two terms, i.e., the approximation error term C_1 and C_2 during the E -th epoch.

Recalling Lemma 2, we have that for all $t = eB + b$,

$$\|\Delta_{e,b}^{-u}\| = \|\mathbf{w}_{e,b}^{-U} - \mathbf{w}_{e,b}\| \leq 2\eta C \frac{1 - q^t}{1 - q}. \tag{37}$$

Recalling Lemma 3, we have that for all e, b and ρ is the spectral radius of $\mathbf{I} - \frac{\eta_{e,b}}{|\mathcal{B}_{e,b}|} \mathbf{H}_{e,b}$,

$$\|\hat{\mathbf{H}}_{e,b} \Delta_{e,b}^{-u}\| = \left\| \left(\mathbf{I} - \frac{\eta_{e,b}}{|\mathcal{B}_{e,b}|} \mathbf{H}_{e,b} \right) \Delta_{e,b}^{-u} \right\| \leq \rho \|\Delta_{e,b}^{-u}\| \leq \rho \cdot 2\eta C \frac{1 - q^t}{1 - q}, \tag{38}$$

Therefore, we can bound the approximation error terms C_1 and C_2 during the E -th epoch as follows:

(1) we first bound the first approximation error term C_1 during the E -th epoch. For clarity, We define T as the total number of steps of SGD updates performed when obtaining $\mathbf{a}_{E,B}$, where $T = EB + B$.

$$\begin{aligned}
&q^{T-1} \|\Delta_{E,B-1}^{-u}\| + q^{T-2} \|\hat{\mathbf{H}}_{E,B-1} \Delta_{E,B-2}^{-u}\| + \dots + q^{T-B} \left\| \prod_{b=0}^{B-1} \hat{\mathbf{H}}_{E,b} \Delta_{E,0}^{-u} \right\| \\
&\leq 2\eta C \frac{q^{T-1} - q^{2(T-1)}}{1 - q} + 2\eta C \frac{q^{T-2} - q^{2(T-2)}}{1 - q} \rho + \dots + 2\eta C \frac{q^{T-B} - q^{2(T-B)}}{1 - q} \rho^{B-1} \tag{39} \\
&= \frac{2\eta C}{1 - q} \sum_{k=T-1}^{T-B} \rho^{T-1-k} (q^k - q^{2k}).
\end{aligned}$$

(2) we then bound the second approximation error term C_2 during the E -th epoch. We threshold the stochastic gradient norm $\|\nabla \ell(\mathbf{w}_{e,b}; u)\|$ at C when clipping is applied, and we thus have the following upper bound,

$$\frac{\eta q^{T-B+b(u)}}{|\mathcal{B}_{E,b(u)}|} \left\| \prod_{b=b(u)+1}^{B-1} \hat{\mathbf{H}}_{E,b} (\nabla \ell(\mathbf{w}_{E,b(u)}^{-u}; u) - \nabla \ell(\mathbf{w}_{E,b(u)}; u)) \right\| \leq \frac{2C\eta}{|\mathcal{B}|} q^{T-B+b(u)} \rho^{B-b(u)-1}. \tag{40}$$

Similarly, for each epoch, we have the aforementioned approximation error bound. Moreover, it is noted that when $e = 0$, the initial models for the retraining process and the learning process are same.

Therefore, we have the following overall approximate error across all epochs:

$$\begin{aligned}
& \|\mathbf{w}_{E,B}^{-u} - \mathbf{w}_{E,B} - \mathbf{a}_{E,B}^{-u}\| \\
& \leq \eta \left(q^{T-1} \|\Delta_{E,B-1}^{-u}\| + q^{T-2} \|\hat{\mathbf{H}}_{E,B-1} \Delta_{E,B-2}^{-u}\| + \dots + q^0 \prod_{k=0}^{E-1} \prod_{b=0}^{B-1} \hat{\mathbf{H}}_{k,b} \Delta_{0,0}^{-u} \right) \\
& \quad + \frac{\eta q^{T-B+b(u)}}{|\mathcal{B}_{E,b(u)}|} \left\| \prod_{b=b(u)+1}^{B-1} \hat{\mathbf{H}}_{E,b} (\nabla \ell(\mathbf{w}_{E,b(u)}^{-u}; u) - \nabla \ell(\mathbf{w}_{E,b(u)}; u)) \right\| + \dots \\
& \quad + \frac{\eta q^{b(u)}}{|\mathcal{B}_{0,b(u)}|} \left\| \prod_{e=0}^E \prod_{b=b(u)+1}^{B-1} \hat{\mathbf{H}}_{E,b} (\nabla \ell(\mathbf{w}_{0,b(u)}^{-u}; u) - \nabla \ell(\mathbf{w}_{0,b(u)}; u)) \right\| \tag{41} \\
& \leq 2\eta^2 C \frac{q^{T-1} - q^{2(T-1)}}{1-q} + 2\eta^2 C \frac{q^{T-2} - q^{2(T-2)}}{1-q} \rho + \dots + 2\eta^2 C \frac{q^0 - q^{2 \times (0)}}{1-q} \rho^{T-1} \\
& \quad + \frac{2C\eta}{|\mathcal{B}|} q^{T-B+b(u)} \rho^{B-b(u)-1} + \dots + \frac{2C\eta}{|\mathcal{B}|} q^{b(u)} \rho^{T-b(u)-1} \\
& = \frac{2\eta^2 C}{1-q} \sum_{k=0}^{T-1} \rho^{T-k-1} (q^k - q^{2k}) + \frac{2C\eta}{|\mathcal{B}|} \sum_{e=0}^E \rho^{T-eB-b(u)-1} q^{eB+b(u)}.
\end{aligned}$$

Through the polynomial multiplies geometric progression, we obtain,

$$\begin{aligned}
\|\mathbf{w}_{E,B}^{-u} - \mathbf{w}_{E,B} - \mathbf{a}_{E,B}^{-u}\| & = \frac{2\eta^2 C}{1-q} \sum_{k=0}^{T-1} \rho^{T-k-1} (q^k - q^{2k}) + \frac{2C\eta}{|\mathcal{B}|} \sum_{e=0}^E \rho^{T-eB-b(u)-1} q^{eB+b(u)} \\
& = \frac{2\eta^2 C}{1-q} \rho^{T-1} \sum_{k=0}^{T-1} \left(\left(\frac{q}{\rho}\right)^k - \left(\frac{q^2}{\rho}\right)^k \right) + \frac{2C\eta}{|\mathcal{B}|} \rho^{T-b(u)-1} q^{b(u)} \sum_{e=0}^E \left(\frac{q}{\rho}\right)^{eB} \\
& = \frac{2\eta^2 C}{1-q} \left(\frac{\rho^T - q^T}{\rho - q} - \frac{\rho^T - q^{2T}}{\rho - q^2} \right) + \frac{2C\eta}{|\mathcal{B}|} \frac{\rho^T - q^T}{\rho^B - q^B} \rho^{B-b(u)-1} q^{b(u)}. \tag{42}
\end{aligned}$$

For convenience, we define $\zeta_T^{-u} = \frac{\eta}{1-q} \left(\frac{\rho^T - q^T}{\rho - q} - \frac{\rho^T - q^{2T}}{\rho - q^2} \right) + \frac{1}{|\mathcal{B}|} \frac{\rho^T - q^T}{\rho^B - q^B} \rho^{B-b(u)-1} q^{b(u)}$. At this point, we have completed the proof of [Theorem 4](#) as follows,

$$\|\mathbf{w}_{E,B}^{-u} - \mathbf{w}_{E,B} - \mathbf{a}_{E,B}^{-u}\| \leq 2\eta C \zeta_T^{-u}. \tag{43}$$

Note that $2\eta C$ is a small constant. Therefore, when $\rho < 1$ (e.g. [Assumption 1](#)), where T is sufficiently large, the error tends towards zero. That is, the unlearned model can almost be equivalent to the retrained model without the need for retraining. \square

B.5 Additional Definitions

We provide the following standard definitions of λ -strong convexity, L -Lipschitzness, M -Smoothness.

Definition 2 (λ -Strong convexity). *The loss function $\ell(\mathbf{w}; z)$ is λ -strongly convex, i.e., there exists a constant $\lambda > 0$ such that for any $z \in \mathcal{Z}$ and $\mathbf{w}_1, \mathbf{w}_2 \in \mathbb{R}^d$, it holds that*

$$\ell(\mathbf{w}_1; z) \geq \ell(\mathbf{w}_2; z) + \langle \nabla \ell(\mathbf{w}_2; z), \mathbf{w}_1 - \mathbf{w}_2 \rangle + \frac{\lambda}{2} \|\mathbf{w}_1 - \mathbf{w}_2\|^2, \tag{44}$$

or equivalently, $\|\nabla \ell^2(\mathbf{w}; z)\| \geq \lambda$ for all $\mathbf{w} \in \mathbb{R}^d$.

Definition 3 (L -Lipschitzness). *The loss function $\ell(\mathbf{w}; z)$ is L -Lipschitz, i.e., there exists a constant $L > 0$ such that for any $z \in \mathcal{Z}$ and $\mathbf{w}_1, \mathbf{w}_2 \in \mathbb{R}^d$, it holds that*

$$|\ell(\mathbf{w}_1; z) - \ell(\mathbf{w}_2; z)| \leq L \|\mathbf{w}_1 - \mathbf{w}_2\|. \tag{45}$$

or equivalently, $\|\nabla \ell(\mathbf{w}; z)\| \leq L$ for all $\mathbf{w} \in \mathbb{R}^d$.

Definition 4 (M -Smoothness or gradient-Lipschitzness). *The loss function $\ell(\mathbf{w}; z)$ is M -smooth, i.e., there exists a constant $M > 0$ such that for any $z \in \mathcal{Z}$ and $\mathbf{w}_1, \mathbf{w}_2 \in \mathbb{R}^d$, it holds that*

$$\|\nabla \ell(\mathbf{w}_1; z) - \nabla \ell(\mathbf{w}_2; z)\| \leq M \|\mathbf{w}_1 - \mathbf{w}_2\|, \tag{46}$$

or equivalently, $\|\nabla \ell^2(\mathbf{w}; z)\| \leq M$ for all $\mathbf{w} \in \mathbb{R}^d$.

B.6 Detailed Proof of Theorem 5

Before we commence with our proof, we present some necessary lemmata.

Lemma 6 (Shalev-Shwartz et al. [46]). *Let \mathbf{w}^* denote a minimizer of the population risk in (1) and $\hat{\mathbf{w}}^{-U}$ denote a minimizer of the empirical risk without the knowledge of U in (2) which aims to minimize $F_{S \setminus U}(\mathbf{w})$, where $|U| = m$. For λ -strongly convex and L -lipschitz objectives, we have,*

$$\mathbb{E} [F(\hat{\mathbf{w}}^{-U}) - F(\mathbf{w}^*)] \leq \frac{4L^2}{\lambda(n-m)}. \quad (47)$$

Proof of Lemma 6. A comprehensive proof of Lemma 6 is available in [46]. \square

Lemma 7. *For any $z \in \mathcal{Z}$, the loss function $\ell(\mathbf{w}; z)$ is λ -strongly convex, L -Lipschitz and M -smooth. Let $\hat{\mathbf{w}}^{-U} = \operatorname{argmin}_{\mathbf{w}} F_{S \setminus U}(\mathbf{w})$ without the knowledge of U in problem (2). For all e, b and vector $\mathbf{v} \in \mathbb{R}^d$, the spectral radius of $\mathbf{I} - \frac{\eta_{e,b}}{|\mathcal{B}_{e,b}|} \mathbf{H}_{e,b}$ is defined as ρ which is largest absolute eigenvalue of these matrices. We have that after T steps of GD with initial stepsize $\eta \leq \frac{2}{\lambda+M}$,*

$$\|\mathbf{w}_T^{-U} - \hat{\mathbf{w}}^{-U}\| \leq \rho^T \frac{2M}{\lambda}, \text{ where } \rho = \max\{|1 - \eta\lambda|, |1 - \eta M|\} < 1. \quad (48)$$

Proof of Lemma 7. Recalling that, according to the strong convexity and smoothness, $\lambda, M > 0$, we have $\lambda \mathbf{I} \preceq \nabla^2 \ell(\mathbf{w}; z) \preceq M \mathbf{I}$. Therefore, we have

$$(1 - \eta_T \lambda) \mathbf{I} \preceq \mathbf{I} - \frac{\eta_T}{|\mathcal{B}_T|} \sum_{i \in \mathcal{B}_T} \nabla^2 \ell(\mathbf{w}_T^{-U}; z_i) \preceq (1 - \eta_T M) \mathbf{I}. \quad (49)$$

Let $\eta \leq \frac{2}{\lambda+M}$. Therefore, $\eta_T \leq \frac{2}{\lambda+M}$, which implies that for any $T \geq 0$:

$$|1 - \eta_T \lambda| < 1, \quad |1 - \eta_T M| < 1. \quad (50)$$

It is seen from the fundamental theorem of calculus that

$$\nabla F_{S \setminus U}(\mathbf{w}_T^{-U}) = \nabla F_{S \setminus U}(\mathbf{w}_T^{-U}) - \underbrace{\nabla F_{S \setminus U}(\hat{\mathbf{w}}^{-U})}_{=0} = \left(\int_0^1 \nabla^2 F_{S \setminus U}(\mathbf{w}_\tau^{-U}) d\tau \right) (\mathbf{w}_T^{-U} - \hat{\mathbf{w}}^{-U}), \quad (51)$$

where $\mathbf{w}_\tau^{-U} := \mathbf{w}_T^{-U} + \tau(\hat{\mathbf{w}}^{-U} - \mathbf{w}_T^{-U})$. Here, $\{\mathbf{w}_\tau^{-U}\}_{0 \leq \tau \leq 1}$ forms a line segment between \mathbf{w}_T^{-U} and $\hat{\mathbf{w}}^{-U}$. Therefore, According to the GD update rule and based on Lemma 3, we have,

$$\begin{aligned} \|\mathbf{w}_{T+1}^{-U} - \hat{\mathbf{w}}^{-U}\| &= \left\| \left(\mathbf{I} - \eta_T \int_0^1 \nabla^2 F_{S \setminus U}(\mathbf{w}_\tau^{-U}) d\tau \right) (\mathbf{w}_T^{-U} - \hat{\mathbf{w}}^{-U}) \right\| \\ &\leq \sup_{0 \leq \tau \leq 1} \|\mathbf{I} - \eta_T \nabla^2 F_{S \setminus U}(\mathbf{w}_\tau^{-U})\| \|\mathbf{w}_T^{-U} - \hat{\mathbf{w}}^{-U}\| \leq \rho \|\mathbf{w}_T^{-U} - \hat{\mathbf{w}}^{-U}\|. \end{aligned} \quad (52)$$

Apply it recursively,

$$\|\mathbf{w}_T^{-U} - \hat{\mathbf{w}}^{-U}\| \leq \rho^T \|\mathbf{w}_0^{-U} - \hat{\mathbf{w}}^{-U}\|, \text{ where } \rho = \max\{|1 - \eta\lambda|, |1 - \eta M|\} < 1. \quad (53)$$

By the assumption that λ -strongly convex and L -Lipschitzness, which implies that

$$\begin{aligned} \frac{\lambda}{2} \|\mathbf{w}^{-U} - \hat{\mathbf{w}}^{-U}\|^2 &\leq F(\mathbf{w}^{-U}) - F(\hat{\mathbf{w}}^{-U}) \\ F(\mathbf{w}^{-U}) - F(\hat{\mathbf{w}}^{-U}) &\leq \frac{2L^2}{\lambda}. \end{aligned} \quad (54)$$

Therefore, we have completed the proof as follows,

$$\|\mathbf{w}_T^{-U} - \hat{\mathbf{w}}^{-U}\| \leq \rho^T \frac{2L}{\lambda}, \text{ where } \rho = \max\{|1 - \eta\lambda|, |1 - \eta M|\} < 1. \quad (55)$$

\square

Building upon the proofs presented in Lemma 6 and Lemma 7, we are now prepared to establish the generalization results stated in Theorem 5.

Proof of Theorem 5. Let $\hat{\mathbf{w}}^{-U}$ be the empirical risk minimizer of the objective function $F_{S \setminus U}(\mathbf{w})$, where $|U| = m$. Let T be the total number of update steps. For any $z \in \mathcal{Z}$ the loss function $\ell(\mathbf{w}; z)$ is λ -strongly convex, M -smoothness and L -Lipschitz. For a minimizer \mathbf{w}^* of the population risk in (1) and $\tilde{\mathbf{w}}_{E,B}^{-U} = \mathbf{w}_{E,B} + \mathbf{a}_{E,B}^{-U} + \sigma$, we have that

$$\mathbb{E} [F(\tilde{\mathbf{w}}_{E,B}^{-U}) - F(\mathbf{w}^*)] = \mathbb{E} [F(\tilde{\mathbf{w}}_{E,B}^{-U}) - F(\hat{\mathbf{w}}^{-U})] + \mathbb{E} [F(\hat{\mathbf{w}}^{-U}) - F(\mathbf{w}^*)]. \quad (56)$$

Based on Lemma 6, we get

$$\mathbb{E} [F(\hat{\mathbf{w}}^{-U}) - F(\mathbf{w}^*)] \leq \frac{4L^2}{\lambda(n-m)}. \quad (57)$$

Then we note that the function $F(\mathbf{w})$ satisfies L -Lipschitz, therefore we can obtain,

$$\mathbb{E} [F(\tilde{\mathbf{w}}_{E,B}) - F(\mathbf{w}^*)] \leq \mathbb{E}[L\|\tilde{\mathbf{w}}_{E,B} - \hat{\mathbf{w}}^{-U}\|] + \frac{4L^2}{\lambda(n-m)}. \quad (58)$$

For the first term of (58), we have

$$\mathbb{E} [\|\tilde{\mathbf{w}}_{E,B}^{-U} - \mathbf{w}_{E,B}^{-U} + \mathbf{w}_{E,B}^{-U} - \hat{\mathbf{w}}^{-U}\|] \leq \underbrace{\mathbb{E}[\|\tilde{\mathbf{w}}_{E,B}^{-U} - \mathbf{w}_{E,B}^{-U}\|]}_{C_3} + \underbrace{\mathbb{E}[\|\mathbf{w}_{E,B}^{-U} - \hat{\mathbf{w}}^{-U}\|]}_{C_4}. \quad (59)$$

Therefore, we now bound the first term C_3 and the second term C_4 of (59) as follows:

(1) C_4 : Based on Lemma 7 and $\mathbf{w}_{E,B}^{-U} = \mathbf{w}_T^{-U}$, we have that for $\eta \leq \frac{2}{\lambda+M}$,

$$\mathbb{E}[\|\mathbf{w}_{E,B}^{-U} - \hat{\mathbf{w}}^{-U}\|] \leq \rho^T \frac{2L}{\lambda}, \quad (60)$$

where $\rho = \max\{|1 - \eta\lambda|, |1 - \eta M|\} < 1$.

(2) C_3 : Based on Theorem 4, we obtain,

$$\begin{aligned} \mathbb{E}[\|\tilde{\mathbf{w}}_{E,B}^{-U} - \mathbf{w}_{E,B}^{-U}\|] &= \mathbb{E}[\|\mathbf{w}_{E,B} + \mathbf{a}_{E,B}^{-U} - \mathbf{w}_{E,B}^{-U}\|] + \mathbb{E}[\|\sigma\|] \\ &\leq 2\eta C \zeta_T^{-U} + \sqrt{dc}. \end{aligned} \quad (61)$$

$$\text{where } \zeta_T^{-U} = \mathcal{O}\left(\frac{\rho^T - q^T}{\rho - q} - \frac{\rho^T - q^{2T}}{\rho - q^2} + \frac{\rho^T - q^T}{\rho^B - q^B}\right).$$

And since the loss function $\ell(\mathbf{w}; z)$ satisfies M -smoothness and λ -strongly convex, we thus have that $0 < \rho < 1$. Plugging the above bound (60) and (61) into (59), we have

$$\mathbb{E} [F(\tilde{\mathbf{w}}_{E,B}^{-U}) - F(\mathbf{w}^*)] \leq \rho^T \frac{2L^2}{\lambda} + \left(\frac{\sqrt{d}\sqrt{2\ln(1.25/\delta)}}{\epsilon} + 1\right) \cdot 2L\eta C \zeta_T^{-U} + \frac{4L^2}{\lambda(n-m)}. \quad (62)$$

Therefore, we have completed the proof. \square

Tightness Analysis of Theorem 5. (1) When T is sufficiently large such that the model $\mathbf{w}_{E,B}^{-U}$ is the empirical risk minimizer $\hat{\mathbf{w}}^{-U}$ of the objective function $F_{S \setminus U}(\mathbf{w})$, the first two terms tend towards zero: the first term $\|\mathbf{w}_{E,B}^{-U} - \hat{\mathbf{w}}^{-U}\|$ is zero; In the second term, we observe that $\zeta_T^{-U} = \mathcal{O}\left(\frac{\rho^T - q^T}{\rho - q} - \frac{\rho^T - q^{2T}}{\rho - q^2} + \frac{\rho^T - q^T}{\rho^B - q^B}\right)$, and as T is sufficiently large, the error tends towards zero.

(2) Furthermore, the following settings, where the model does not converge and ρ is close to q , might render the bound on the approximation error vacuous and also lead to high approximation error. We note that the first and third terms of ζ_T^{-U} can be equivalently written as $\frac{\rho^T - q^T}{\rho - q} + \frac{\rho^T - q^T}{\rho^B - q^B} = \rho^{T-1} \sum_{t=0}^{T-1} \left(\frac{q}{\rho}\right)^t + \rho^{T-B} \sum_{e=0}^B \left(\frac{q}{\rho}\right)^{eB}$. These terms increase as ρ approaches q , however are always upper bounded by $\rho^{T-1} \cdot T + \rho^{T-B} \cdot T$. In our analysis, $T = EB + B$ is a fixed constant, so this upper bound remains meaningful, although it may not be tight in some cases.

C Supplementary Experiments

The experiments were conducted on the NVIDIA GeForce RTX 4090 (3090). The code were implemented in PyTorch 2.0.0 and leverage the CUDA Toolkit version 11.8. Our comprehensive tests were conducted on AMD EPYC 7763 CPU @ 1.50GHz with 64 cores under Ubuntu20.04.6 LTS. Source Code: <https://github.com/Anonymous202401/If-Recollecting-were-Forgetting>

C.1 Additional Verification Experiments

The verification experiments in this section consist of two parts: (1) We first investigate the reasons behind the randomness of previous works under the non-convex setting. We select forgetting samples under different random seeds, and show that previous works exhibit dependence for forgetting samples, meaning that the forgetting effect of previous works is beneficial for some samples but poor for others. (2) Secondly, we conduct experiments on larger-scale dataset and model with more metrics, which previous works could not achieve because the computation of the Hessian is expensive. This demonstrates the potential of our proposed hessian-free method on large-scale models and datasets.

Sensitivity to the forgetting samples. We conduct experiments on a simple CNN and the hyper-parameter setup is consistent with the verification experiments I in the main paper. As shown in Figure 2, we provide intuitive insights into the reasons for the decline of prior works in non-convex settings. Specifically, we investigated the L_2 norm of the approximate parameter change $\|\mathbf{a}^{-U}\|$ and the norm of the exact parameter change $\|\mathbf{w}_{E,B}^{-U} - \mathbf{w}_{E,B}\|$ across different selections of the forgetting sample. We observed that the performance of NS and IJ depends on the selection of the forgetting data, i.e., they can approximate actual changes well for some data points while generating large approximation errors for others under the non-convex setting, as illustrated in Figure 2. The dependency of forgetting data results in the decrease in distance and correlation coefficient metrics observed in Figure 1 (b). The observed results for NS and IJ are consistent with previous studies on influence functions [35, 42], where these methods display random behavior under the non-convex setting, resulting in a decrease in correlation with retraining. In contrast, our approach can effectively approximate the actual norm of parameter changes, regardless of the forgetting sample selection.

Additional Experiments. We further evaluate using a larger-scale model (ResNet-18 [47]) which features 11 M parameters with three different datasets: CIFAR-10 [48] for image classification, CelebA [49] for gender prediction, and the LFWPeople [50] for face recognition across 29 different individuals. Since prior second-order works NS [2] and IJ [3] are difficult to compute (Hessian) in this scenario, we instead use the following baselines, as described and similarly set up in [25]:

- *FineTune*: In case of finetuning, the original learned model is finetuned on the remaining dataset.
- *NegGrad*: In case of gradient ascent, the learned model is finetuned using the negative of update direction on the forgetting dataset.

Configurations: (1) We conducted evaluation on ResNet-18 trained on CIFAR-10 with 50,000 samples. The learning stage is conducted for 40 epochs with a stepsize of 0.001 and a batch size of 256. For FineTune, 10 epochs of training are performed with a step size of 0.001 and a batch size of 256. For NegGrad, we run gradient ascent for 1 epoch with a step size of 5×10^{-5} and a batch size of 2. (2) We conducted evaluation on ResNet-18 trained on LFW with 984 samples, for the classification of 29 facial categories. The learning stage is conducted for 49 epochs with a stepsize of 0.004 and a batch size of 41. For FineTune, 10 epochs of training are performed with a step size of 0.004 and a batch size of 41. For NegGrad, we run gradient ascent for 1 epochs with a step size of 4×10^{-6} and a batch size of 1. (3) We conducted evaluation on ResNet-18 trained on CelebA with

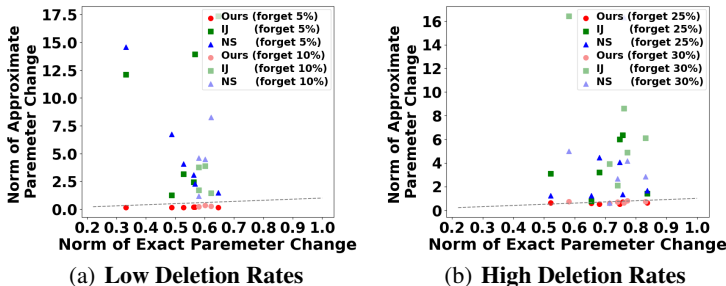


Figure 2: **Verification experiments II.** Evaluation shows a comparison comparison between the norm of approximate parameter change $\|\mathbf{a}^{-U}\|$ and norm of exact parameter change $\|\mathbf{w}_{E,B}^{-U} - \mathbf{w}_{E,B}\|$ across different random seeds. Intuitively, the NS and IJ methods are contingent on the selection of forgetting data. In contrast, our approach consistently approximates the actual values effectively.

10,000 samples. The learning stage is conducted for 5 epochs with a stepsize of 0.01 and a batch size of 64. For FineTune, 2 epochs of training are performed with a step size of 0.01 and a batch size of 64. For NegGrad, we run gradient ascent for 1 epoch with a step size of 0.0005 and a batch size of 1. Finally, we uniformly unlearned 50 data points for each dataset. We define D_t as the test dataset, D_r as the remaining dataset, and D_f as the forgetting dataset.

The following Table 3-5 are our evaluation results: we employ five widely-used metrics to evaluate the performance of unlearning methods: Acc_{D_t} (accuracy on D_t), $error_{D_t}$ (error on D_t), $error_{D_r}$ (error on D_r), $error_{D_f}$ (error on D_f), $dis.$ (L_2 distance between the unlearned and retrained model).

Performances of our Scheme: We still maintain model indistinguishability and accuracy indistinguishability from the retrained model on more complex tasks and larger models, where the distance is only 0.06 on CIFAR10 and 0.29 on CelebA. The results also shows that the unlearned model of proposed method performs similarly to the retrained model in terms of the accuracy metric. Moreover, compared to these baselines, our method achieves forgetting in only millisecond-level due to the pre-computation of all statistical data, demonstrating the potential of our method on larger-scale models. Additionally, we noticed that when training is unstable, our method would lead to larger performance degradation, such as on the LFW dataset. Although our method has similar accuracy on the forgetting dataset, it suffers performance loss on the remaining dataset. This implies that our method is sensitive to the training process and hyperparameters in non-convex scenarios. We summarize the limitations in Appendix E.2, and provide possible schemes to address these problems.

Model indistinguishability: For FineTune, we can observe that even though the accuracy results are similar to the retrained model, the distance metric is very large (e.g. 2.21 on CIFAR-10 and 2.36 on CelebA). For NegGrad, we observe that the accuracy on forgetting dataset D_f and remaining dataset D_r would rapidly decrease simultaneously, but even in this case, the distances are still lower than that of FineTune for all three datasets. This demonstrates that a small difference in accuracy does not indicate the model indistinguishability. Therefore, we use the L_2 norm and correlation metric as the primary measure of forgetting completeness, which are commonly employed in studies related to *influence function* [35, 42]. These studies serve as inspiration for prior theoretical certified unlearning works [2, 3, 4] that we compare. Measuring forgetting through L_2 norm is one of the most stringent metrics and is also used in unlearning research, e.g., [15, 18], but it necessitates retraining a model, which is impractical for real-world applications. Therefore, exploring more effective and efficient metrics to evaluate model indistinguishability is an interesting and important topic in the future.

Table 3: **Verification experiments III.** Unlearning results on Resnet-18 trained on CIFAR-10 dataset.

Method	Acc_{D_t} (%)	Err_{D_t} (%)	Err_{D_r} (%)	Err_{D_f} (%)	$Dis.$	Runtime (Sec)
FineTune	79.34	20.66	15.92	22.00	2.21	106.76
NegGrad	40.61	59.39	59.15	70.00	0.11	0.56
Retrain	79.63	20.37	16.19	24.00	—	468.65
Ours	79.62	20.38	16.15	22.00	0.06	0.0006

Table 4: **Verification experiments IV.** Unlearning results on Resnet-18 trained on LFW dataset.

Method	Acc_{D_t} (%)	Err_{D_t} (%)	Err_{D_r} (%)	Err_{D_f} (%)	$Dis.$	Runtime (Sec)
FineTune	76.02	23.98	8.99	4.00	0.52	15.60
NegGrad	63.01	36.99	15.63	20.00	0.48	0.46
Retrain	80.89	19.11	4.07	26.00	—	77.43
Ours	71.92	28.08	14.91	22.00	0.33	0.001

Table 5: **Verification experiments V.** Unlearning results on Resnet-18 trained on CelebA dataset.

Method	Acc_{D_t} (%)	Err_{D_t} (%)	Err_{D_r} (%)	Err_{D_f} (%)	$Dis.$	Runtime (Sec)
FineTune	95.78	4.22	1.07	4.00	2.36	35.09
NegGrad	37.95	62.05	58.12	60.0	1.13	0.96
Retrain	95.72	4.28	1.20	4.00	—	87.72
Ours	95.57	4.43	1.12	2.00	0.29	0.0006

C.2 Additional Application Experiments

Furthermore, we evaluate the performance on different datasets and models in real-world application. Our evaluations are conducted from two perspectives: runtime and utility. Specifically, run-time focuses on the time spent precomputing unlearning statistics and the speedup of the unlearning algorithm compared to the retraining algorithm. Moreover, we evaluate the utility by the test accuracy of the unlearned model to ensure that generalization performance is not compromised.

Configurations: We assess the performance on various datasets and models, as presented in Table 6-Table 7. The values in parentheses indicate the difference in test accuracy compared to the retrained model. (1) We train a LR and simple CNN on MNIST with 1,000 data points with 20% data to be forgotten, which have setups identical to the aforementioned verification experiments I. We further simulate on FMNIST with 4,000 data using CNN and LeNet with total 61,706 parameters. The training is conducted for 30 epochs with stepsize of 0.5 and a batch size of 256. (2) Moreover, we assessed our method on Resnet-18 [47] trained on the CIFAR10 dataset for image classification with 50,000 data points, CelebA dataset for gender prediction with 10,000 data points, and LFWPeople dataset for face recognition with 984 data points. The hyperparameter configurations align with those detailed in Table 3-5. In these circumstances, we have not evaluated NS and IJ due to out-of-memory.

Application experiment results show that our proposed method is computationally efficient and performs well in realistic environments, outperforming benchmarks of certified unlearning regarding all metrics by a significant margin, as demonstrated in Table 6. It achieves minimal computational and storage overhead while maintaining high performance in both convex and non-convex settings. We further investigate data removal with large-scale datasets using ResNet-18, as shown in Table 7. Our proposed Hessian-free method demonstrates significant potential for over-parameterized models, as previous second-order certified unlearning works are unable to compute the full Hessian matrix in such cases. Notably, for unlearning runtime, by precomputing statistical data before unlearning requests arrive, we only need to execute simple vector additions, achieving millisecond-level efficiency (0.6 ms) with minimal performance degradation in test accuracy.

Finally, although our method has lower computation and storage complexity compared to previous works, it still requires $\mathcal{O}(nTd)$ precomputation and $\mathcal{O}(nd)$ storage which is expensive when facing both larger-scale models and datasets. We summarize the limitations in Appendix E.2, and provide possible schemes to address these problems.

Table 6: **Application experiments II.** An online scenario on small-scale datasets and models, where the unlearning requests involve only forgetting a single data point with each execution. We compute the total computational/storage cost for all samples and tested the accuracy of final unlearned model.

Method	Dataset	Model	Unlearning Computaion		PreComputaion Runtime (Sec)	Storage (GB)	Dis.	Test Accuracy (%) Unlearned model
			Runtime (Sec)	Speedup				
NS	MNIST	Logistic	5.14×10^2	$2.39 \times$	2.57×10^3	0.23	0.13	87.50 (-0.75)
		CNN	5.82×10^3	$0.05 \times$	2.91×10^4	1.78	1.78	83.50 (-10.25)
	FMNIST	CNN	2.31×10^4	$0.54 \times$	1.16×10^5	1.78	2.41	57.69 (-22.25)
		LeNet	8.53×10^4	$0.15 \times$	4.27×10^5	14.18	1.10	62.00 (-18.50)
IJ	MNIST	Logistic	1.84×10^0	$665 \times$	2.57×10^3	0.25	0.13	87.50 (-0.75)
		CNN	6.81×10^0	$45 \times$	2.91×10^4	1.78	3.12	82.75 (-11.00)
	FMNIST	CNN	2.95×10^1	$424 \times$	1.16×10^5	1.78	0.94	75.69 (-4.25)
		LeNet	3.24×10^1	$402 \times$	4.27×10^5	14.18	0.57	76.75 (-3.75)
Ours	MNIST	Logistic	2.74×10^{-3}	$448,060 \times$	1.95×10^1	0.03	0.12	87.75 (-0.50)
		CNN	3.23×10^{-2}	$9,940 \times$	5.34×10^2	0.08	0.68	91.50 (-2.25)
	FMNIST	CNN	1.27×10^{-1}	$98,468 \times$	3.66×10^3	0.32	0.74	77.85 (-2.09)
		LeNet	1.63×10^{-1}	$79,828 \times$	4.43×10^3	0.48	0.53	78.63 (-1.87)

Table 7: **Application experiments III.** An online scenario on the Resnet-18 with large-scale datasets. We compute the computational and cost overhead of per forgetting sample.

Method	Dataset	Unlearning Computaion (per sample)		PreComputaion (per sample) Runtime (Sec)	Storage (per sample) (GB)	Dis.	Test Accuracy (%) Unlearned model
		Runtime (Sec)	Speedup				
Ours	CIFAR10	0.6×10^{-3}	$781,083 \times$	184.53	0.043	0.09	79.62 (-0.01)
	LFW	1.0×10^{-3}	$77,430 \times$	84.99	0.043	0.31	71.92 (-8.97)
	CelebA	0.6×10^{-3}	$146,200 \times$	31.90	0.042	0.29	95.57 (-0.15)

D Ablation Studies

Here, we investigate the sensitivity of the proposed approach to hyperparameters. Specifically, we evaluated the effects of different step sizes, epochs, decay rates of step size, and dataset sizes on proposed approach. We conducted simulations in both convex and non-convex scenarios, using Logistic Regression for the convex case and CNN for the non-convex case, respectively.

Takeaway. Let’s first provide a brief summary for the main results of ablation studies.

- **Impact of Step Sizes.** Firstly, a smaller step size enables our model to be closer to the retrained model. This is because [Theorem 4](#) demonstrates that the approximation error mainly consists of two components: (1) the step size $\eta_{e,b}$ and (2) the maximum eigenvalue λ_1 of $\frac{1}{|\mathcal{B}_{e,b}|} \mathbf{H}_{e,b}$. Therefore, a smaller stepsize $\eta_{e,b}$ constrain the maximum eigenvalue of the matrix $\frac{\eta_{e,b}}{|\mathcal{B}_{e,b}|} \mathbf{H}_{e,b}$, leading to a reduction in the error by decreasing the value of ρ . Moreover, with a small step size, increasing epochs does not lead to significant approximation errors; instead, it exhibits better performance under the distance metric compared to a large stepsize.
- **Impact of Epochs.** Secondly, when the step size is sufficiently small, the approximation error is insensitive and exhibits slow growth with respect to the number of epochs, i.e., excessive iterations in this scenario do not lead to significant errors.
- **Impact of Stepsize Decay Rates.** Thirdly, our results indicate that as the decay rate q decreases, the approximation error diminishes. Specifically, The stepsize decay strategy introduces a bound on approximation error, preventing a continuous increase in error as the size of epochs grows.
- **Impact of Dataset Sizes.** Finally, our numerical findings show that the approximation error reduces with larger dataset sizes. Intuitively, as the dataset size increases, the impact of individual data points on model updates diminishes during training. This is typically reflected in the training process, where with an increase in the dataset size, each batch update is less likely to frequently sample a specific data point. Consequently, the impact of any individual data point on updates between the retrained original models diminishes, leading to a more accurate approximation.

D.1 Impact of Step Sizes

In this section, we investigated (i) the impact of step sizes and (ii) the impact of small step size with more epochs. Additionally, we discussed the connection between sharpness in learning generalization studies and our unlearning method.

Configurations: (i) We investigate the impact of step sizes $\{0.001, 0.005, 0.01, 0.05, 0.1, 0.5\}$ on distance metrics in [Table 8](#) and [Table 9](#). (ii) Furthermore, in [Figure 3](#), to investigate the effect of epochs under small step sizes, LR was trained for 750 epochs and 2000 epochs with a step size of 0.001 (initially 0.05 with 50 epochs). For CNN, training for 50 epochs and 500 epochs with a step size of 0.025 (originally 0.05 with 20 epochs) was performed. Additionally, when the step size is very small (0.001) in LR, the stepsize decay strategy causes premature decay to zero before the model convergence. We thus increased the stepsize decay rate from 0.995 to 1. Subsequent experiments will demonstrate that this leads to an increase in approximation error. Finally, we keep the remaining hyperparameters consistent with verification experiment I.

Impact of step sizes. As shown in [Table 8](#) and [Table 9](#), a smaller step size enables our model to be closer to the retrained model. Specifically, as [Theorem 4](#) demonstrates that, in this process, the error arises from the scaled remainder term, i.e., the term $o(\mathbf{w}_{e,b}^{-u} - \mathbf{w}_{e,b})$ is scaled by the subsequent $\mathbf{M}_{e,b(u)}$, where $\mathbf{M}_{e,b(u)} = \frac{\eta_{e,b(u)}}{|\mathcal{B}_{e,b(u)}|} \prod_{k=e}^E \prod_{b=b(u)+1}^{B-1} \left(\mathbf{I} - \frac{\eta_{k,b}}{|\mathcal{B}_{k,b}|} \mathbf{H}_{k,b} \right)$. Therefore, the approximation error mainly consists of two components: (1) the step size $\eta_{e,b}$ and (2) the maximum eigenvalue λ_1 of $\frac{1}{|\mathcal{B}_{e,b}|} \mathbf{H}_{e,b}$. Therefore, a smaller stepsize η constrain the maximum eigenvalue of the matrix $\frac{\eta_{e,b}}{|\mathcal{B}_{e,b}|} \mathbf{H}_{e,b}$, thereby reducing the spectral radius ρ of the matrix $\mathbf{I} - \frac{\eta_{e,b}}{|\mathcal{B}_{e,b}|} \mathbf{H}_{e,b}$, and finally reducing approximation error.

Furthermore, if the step size is extremely large, it will result in a large spectral radius ρ of the matrix $\mathbf{I} - \frac{\eta_{e,b}}{|\mathcal{B}_{e,b}|} \mathbf{H}_{e,b}$, causing exponential growth in errors, as demonstrated in [Table 8](#) and [Table 9](#) for an initial step size of $\eta = 0.5$. In this scenario, our method leads to a complete breakdown of the model, rendering it unusable. However, it is noteworthy that theoretical predictions [\[51\]](#) and empirical

Table 8: **Impact of Step Sizes** on Convex Setting. Stepsize $\eta = 0.05$ represent hyperparameter choices of previous experiments for LR in our paper. It can be observed that as the step size decreases, our method’s unlearned model becomes closer to the retrained model. (Seed 42)

Stepsize	Distance			
	1%	5%	20%	30%
0.001	0.002	0.005	0.014	0.020
0.005	0.007	0.017	0.046	0.065
0.01	0.010	0.024	0.067	0.097
0.05	0.030	0.060	0.163	0.230
0.1	0.047	0.095	0.250	0.348
0.5	0.800	1.730	12.533	14.825

Table 9: **Impact of Step Sizes** on Non-Convex Setting. Stepsize $\eta = 0.05$ represent hyperparameter choices of previous experiments for CNN in our paper. It can be observed that as the step size decreases, our method’s unlearned model becomes closer to the retrained model. (Seed 42)

Stepsize	Distance			
	1%	5%	20%	30%
0.001	0.001	0.002	0.008	0.012
0.005	0.004	0.015	0.058	0.084
0.01	0.017	0.069	0.257	0.372
0.05	0.167	0.380	0.584	0.825
0.1	0.437	0.795	1.722	2.725
0.5	8E+7	3E+7	2E+8	7E+7

validation [52] suggest that, across all datasets and models, successful training occurs only when optimization enters a stable region of parameter space where $\lambda_1 \cdot \eta \leq 2$. Therefore, achieving good optimization results typically does not require a strategy of using aggressive step sizes.

The connection between learning and unlearning. There is a connection between the sharpness of learning generalization studies and the unlearning method that we propose. Specifically, these studies aim to explore the sharpness of the Hessian of loss function $\frac{1}{|\mathcal{B}_{e,b}|} \mathbf{H}_{e,b}$, and the term ‘sharpness’ refers to the maximum eigenvalue of the Hessian, denoted as λ_1 in some studies, such as [52]. A flat loss space is widely recognized as beneficial for gradient descent optimization, leading to improved convergence. Importantly, [52] demonstrates the central role that λ_1 plays in neural network optimization, emphasizing that maintaining a sufficiently small λ_1 during optimization is a necessary condition for successful training (without causing divergence) at large step sizes. Models which train successfully enter a region where $\lambda_1 \cdot \eta \leq 2$ mid training (or fluctuate just above this bound).

In our work, we leverage the second-order information from the loss Hessian at each iteration during the training process to compute the approximators and achieve forgetting. As indicated in [Theorem 4](#), our analysis indicates that a small λ_1 of the Hessian is beneficial for reducing the approximation error. Therefore, effectively reducing λ_1 during optimization, so that the training enters a flatter region, will not only improve the generalization ability of the learning stage model but also reduce the

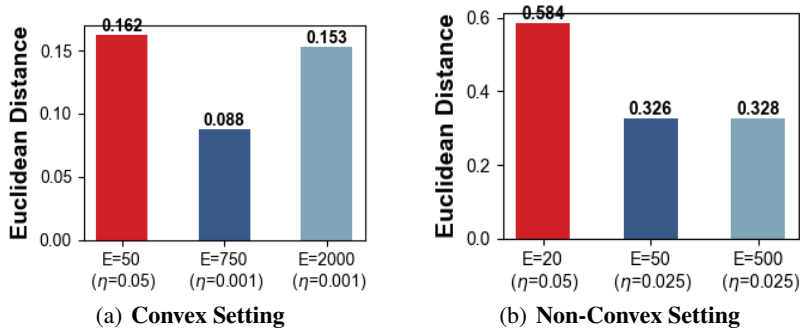


Figure 3: **Impact of Small Step Size with More Epochs.** (a)(b) correspond to LR and CNN with 20% of the data to be forgotten, respectively. The red bar in the left represents the distance metric when using a larger step size; the blue bar in the middle represents the distance metric with a small stepsize during the large epochs; and the right light blue bar in the right represent the distance metric with a small stepsize during the small epochs. It can be observed that smaller step sizes lead to smaller approximation errors. Furthermore, even when training more epochs with smaller step sizes, the approximation error remains lower compared to training with larger learning rates. (Seed 42)

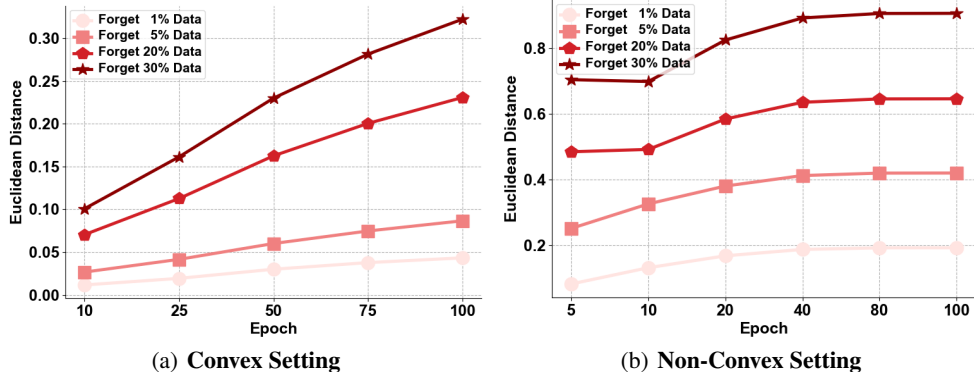


Figure 4: **Impact of Epoch.** (a)(b) illustrate the in the distance metric for LR and CNN by varying epoch from 10 and 100 with 20% data to be forgotten. As shown in the Figure (a)(b), the error accumulates with the increase in epochs. However, with an appropriate choice of step size, such growth is entirely acceptable (Seed 42).

approximation error in the unlearning stage. As suggested in [52], strategies like stepsize warm-up or initialization strategies for architectures can be employed to stabilize learning and potentially reduce unlearning approximation errors by decreasing λ_1 , enabling training at larger step sizes.

Impact of small step size with more epochs. Finally, with a very small step size during model training, we observed a low approximation error. As shown in Figure 3, even as in the case with large epoch sizes, the approximation error remains lower than in the case with a large step size of 0.05. This suggests that a smaller step size reduces the error. It is noted that a smaller step size requires more iterations to converge, resulting in increased computational cost. Therefore, trading an appropriate step size is essential based on different scenarios.

D.2 Impact of Epochs

Our aforementioned experiments indicate that the increase in epochs does not become a major factor affecting approximation errors when applying small step sizes, i.e., with LR at a step size of 0.001 and CNN at a step size of 0.025, the growth of epochs does not significantly impact the approximation error. Conversely, in the case of small step sizes, even as epochs extend to a point where the model approaches overfitting, the error remains lower than scenarios with larger step sizes.

Configurations: Furthermore, we explore the impact of the epoch with a fixed and larger step size, such as the one $\eta = 0.05$ we selected in our study. In this scenario, we evaluate the impact of the epochs on both the distance and accuracy metrics. Specifically, we investigated the distance under the epoch set $\{10, 25, 50, 75, 100\}$ and provided the accuracy on 100 epoch after forgetting 20% data. In addition, the selection of other hyperparameters remains consistent with the ones used previously.

Impact of epochs: In Figure 4, we can observe that the distance slowly increases with the growth of epochs. This is attributed to the fact that each iteration involves an approximation, and multiple rounds of iterations lead to the accumulation on approximation error. However, as Figure 4 shows that, the accumulation of this error is small and does not lead to a significant performance degradation.

D.3 Impact of Decay Rates of Stepsize

This experiments aim to study the impacts of stepsizes. We consider two scenarios: one with stepsize decay ($q = 0.995$) and the other without stepsize decay ($q = 1$).

Impact of decay rates of stepsize: From Figure 5, we can observe that the Euclidean distance for the stepsize decay strategy is generally smaller compared to that without the stepsize decay. This aligns with our earlier analysis of step size in Appendix D.1, i.e., a smaller step size leads to a smaller approximation error and choosing an appropriate stepsize decay rate ensures a continuous reduction in step size, preventing the unbounded growth of the approximation error.

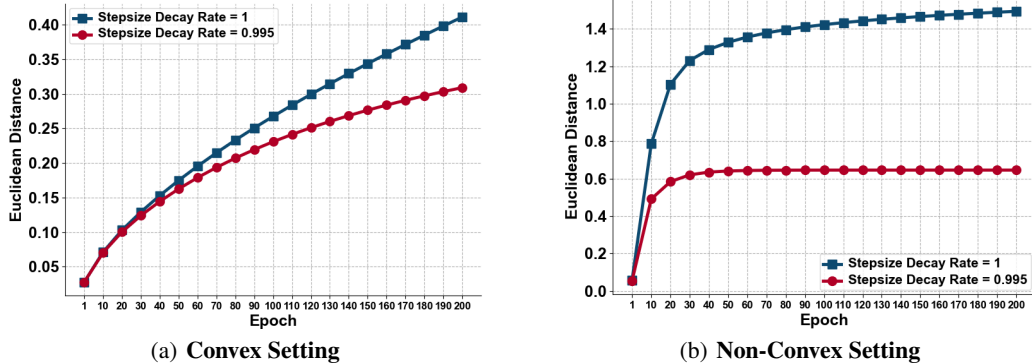


Figure 5: **Impacts of the stepsize decay rate** on the Euclidean distances for (a) the logistic regression and (b) the CNN by varying epochs from 1 to 200. The green line represents learning with a 0.995 stepsize decay rate, while the blue line represents without stepsize decay. It can be observed that stepsize decay effectively reduces the approximation error. (Seed 42)

Additionally, as in Figure 5 (b), we find that the distance of CNN tends to stabilize even without stepsize decay. This result can be explained by the conclusions in [53, 54]. Specifically, [53, 54] analyze the spectral distribution of the Hessian eigenvalues during CNN training. It reveals that, initially, the eigenvalues of Hessian are symmetrically distributed around 0. As training progresses, they converge towards 0, indicating Hessian degeneracy. Towards the end of training, only a small number of eigenvalues become negative and a large portion of the Hessian eigenvalues approach 0 when the training closes to convergence. Let’s recall our previous analysis of stepsize in Appendix D.1, where we demonstrates that the approximation error is primarily determined by ρ of $\mathbf{I} - \frac{\eta_{e,b}}{|\mathcal{B}_{e,b}|} \mathbf{H}_{e,b}$, and ρ is determined by $\eta_{e,b}$ and λ_1 . As the number of iterations increases, the eigenvalues of the loss Hessian $\mathbf{H}_{e,b}$ tends to 0. This implies a decrease in λ_1 , leading to a slower increase in error. Therefore, in Figure 5 (b), the distance gradually stabilizes even without a decay strategy due to the decrease in λ_1 during training, and it still increases due to the existence of some larger outlier eigenvalues.

D.4 Impact of Dataset Sizes

Finally, we assess the impacts of different dataset sizes. To maintain the total number of iterations, we adapt the number of epochs based on the dataset size. We keep other hyperparameters constant. **Impact of dataset sizes:** As shown in Table 10 and Table 11, we observe that larger dataset size generally tends to decrease the approximation error, making the unlearned model more closely resemble the retrained model. A reasonable explanation is that the enlargement of the dataset implies less frequent sampling of a specific sample for updating the model, consequently reducing the impact of data on the model updates in (3). This, in turn, leads to a decrease in the approximation error.

Table 10: **Impact of Dataset Sizes** on Convex Setting. Datasize $n = 1,000$ represent hyperparameter choices of previous experiments for LR in our paper. (Seed 42)

Datasize	Distance			
	1%	5%	20%	30%
500	0.043	0.087	0.212	0.300
1,000	0.030	0.060	0.162	0.230
5,000	0.014	0.036	0.104	0.1521
10,000	0.009	0.028	0.089	0.1334
25,000	0.007	0.024	0.081	0.1195
50,000	0.006	0.022	0.080	0.119

Table 11: **Impact of Dataset Sizes** on Non-Convex Setting. Datasize $n = 1,000$ represent hyperparameter choices of previous experiments for CNN in our paper. (Seed 42)

Datasize	Distance			
	1%	5%	20%	30%
500	0.108	0.237	0.592	0.837
1,000	0.167	0.380	0.584	0.825
2,000	0.092	0.230	0.483	0.715
5,000	0.081	0.177	0.447	0.677
10,000	0.132	0.191	0.463	0.654
20,000	0.165	0.190	0.460	0.617

E Discussion

E.1 Deletion Capacity

We analyze the *deletion capacity* of our method based on the analysis of Sekhari et al. [2], which formalizes how many samples can be deleted from the model parameterized by the original empirical risk minimizer while maintaining reasonable guarantees on the test loss. We establish the relationship between generalization performance and the amount of deleted samples through deletion capacity, and our analysis indicates that our proposed method outperforms previous works in both generalization and deletion capacity. Below, we first formalize the deletion capacity.

Definition 5 (Definition of Deletion Capacity [2]). Let $\varepsilon, \delta \geq 0$. Let S be a dataset of size n drawn i.i.d. from \mathcal{D} , and let $\ell(w; z)$ be a loss function. For a pair of learning and unlearning algorithms $\Omega, \bar{\Omega}$ that are (ε, δ) -unlearning, the deletion capacity $m_{\varepsilon, \delta}^{\Omega, \bar{\Omega}}(d, n)$ is defined as the maximum number of samples U to be forgotten, while still ensuring an excess population risk is γ . Specifically,

$$m_{\varepsilon, \delta, \gamma}^{\Omega, \bar{\Omega}}(d, n) := \max \left\{ m \mid \mathbb{E} \left[\max_{U \subseteq S: |U| \leq m} F(\bar{\Omega}(\Omega(S); T(S)) - F(\mathbf{w}^*)) \right] \leq \gamma \right\}, \quad (63)$$

where the expectation above is with respect to $S \sim \mathcal{D}^n$ and output of the algorithms Ω and $\bar{\Omega}$.

Similar to Sekhari et al. [2], we provide upper bound and lower bound of deletion capacity for our algorithm. We first give the upper bound of deletion capacity.

Theorem 8 (Upper Bound of Deletion Capacity [2]). Let $\delta \leq 0.005$ and $\varepsilon = 1$. There exists a 4-Lipschitz and 1-strongly convex loss function f , and a distribution \mathcal{D} such that for any learning algorithm A and removal mechanism M that satisfies (ε, δ) -unlearning and has access to all remaining samples $S \setminus U$, then the deletion capacity is:

$$m_{\varepsilon, \delta, \gamma}^{A, M}(d, n) \leq cn \quad (64)$$

where c depends on the properties of function f and is strictly less than 1.

A comprehensive proof of [Theorem 8](#) is available in Sekhari et al. [2]. Furthermore, based on [Theorem 5](#), we present the lower bound of deletion capacity below:

Theorem 9 (Lower Bound of Deletion Capacity). There exists a learning algorithm Ω and an unlearning algorithm $\bar{\Omega}$ such that for any convex (and hence strongly convex), L -Lipschitz, and M -Smoothness loss f and distribution \mathcal{D} . Choose step size $\eta \leq \frac{2}{M+\lambda}$ and $\mathbf{w}_{E, B}^{-U}$ is the empirical risk minimizer of objective function $F_{S \setminus U}(\mathbf{w})$, then we have

$$m_{\varepsilon, \delta, \gamma}^{\Omega, \bar{\Omega}}(d, n) \geq n - \frac{4L^2}{\gamma\lambda} \quad (65)$$

Proof of Theorem 9. Based on [Theorem 5](#), we note that $2\eta C$ is a small constant. When T is sufficiently large such that the model $\mathbf{w}_{E, B}^{-U}$ is the empirical risk minimizer $\tilde{\mathbf{w}}^{-U}$ of the objective function $F_{S \setminus U}(\mathbf{w})$, the last two terms thus approach 0. Therefore, we have:

$$F(\tilde{\mathbf{w}}_{E, B}^{-U}) - \mathbb{E}[F(\mathbf{w}^*)] \leq \mathcal{O} \left(\frac{4L^2}{\lambda(n-m)} \right). \quad (66)$$

where $\tilde{\mathbf{w}}_{E, B}^{-U}$ denotes the output point $\bar{\Omega}(\Omega(S); T(S))$ and \mathbf{w}^* is the minimizer of the population risk in (1). Therefore, the above upper bound on the excess risk implies that we can delete at least

$$m = n - \frac{4L^2}{\gamma\lambda} \quad (67)$$

samples while still ensuring an excess risk guarantee of γ . Intuitively, according to [Theorem 5](#), in the optimal situation, we discuss the excess loss of our algorithm and demonstrated its superiority over previous methods, indicating improved deletion capacity. In particular, Sekhari et al. [2] derive the following generalization bound, where $\mathbf{w}_{E, B}$ is required to be the empirical risk minimizer:

$$F(\tilde{\mathbf{w}}_{E, B}^{-U}) - \mathbb{E}[F(\mathbf{w}^*)] \leq \mathcal{O} \left(\frac{mL^2}{\lambda(n-m)} + \sqrt{d}\sigma L + \frac{4L^2}{\lambda n} \right), \quad (68)$$

where σ represents a term associated with noise, while d denotes the dimensionality of the model.

Using the fact that $n = \Omega(m)$, it is noted that in (66), our generalization bound is a constant term of $\frac{L^2}{\lambda(n-m)}$, which was omitted in previous works. This implies that, compared to previous works, our method achieves better generalization results and improved deletion capacity under same assumption (e.g. λ -strongly convex, L -Lipschitz, and M -Smoothness of the objective function, as well as the model being the empirical risk minimizer). \square

E.2 Limitation and Future Work

Compared to prior certified unlearning works, our paper is the first to achieve *near-instantaneous* certified unlearning under *non-convex non-smooth* settings (Theorem 1), and under the same convex and smooth assumptions, our method provides better generalization, deletion capacity, and unlearning guarantees (Theorem 5) than previous works. Moreover, we theoretically (Subsection 4.4) and experimentally (Appendix C.2) demonstrate that our method is more efficient in terms of precomputation/storage and unlearning time complexity than previous approaches.

Although we have made the above contributions, there are still some significant limitations:

1. Firstly, our proposed algorithm necessitates $\mathcal{O}(nTd)$ and $\mathcal{O}(nd)$, which remains costly, particularly in scenarios involving extensive data and larger-scale models. Consequently, conducting experiments concurrently with both large-scale datasets and models is anticipated to significantly extend the time required for precomputing unlearning statistics.
2. In addition, although we establish the analysis of certified unlearning for non-convex scenarios, as demonstrated by the results in Theorem 4, it is important to recognize that the proposed method is highly sensitive to both the experiment’s hyperparameters and the stability of the training process in non-convex settings. If the training process is unstable, our method will obtain a significant approximation error. For example, in Appendix D.1 (in Table 9), when using an aggressive step size (e.g. step size increasing from 0.1 to 0.5), the approximation error becomes very large (with results to the power of 7).

Future work. Therefore, in order to solve the problems mentioned above, we briefly propose some solutions. Specifically, our proposed framework offers the feasibility to unlearn an arbitrary subset of the entire datasets, allowing a trade-off that further reduces the storage complexity, for instance, consider a typical federated unlearning scenario at the user level, where there are k users ($k \ll n$). By focusing on the unlearning of a single user’s dataset or a subset of users’ datasets, we can maintain k vectors for k users’ dataset instead of maintaining n vectors for n all data points. Therefore, we can further reduce storage to $\mathcal{O}(kd)$. Besides, batching is also beneficial for GPU parallel computation.

Furthermore, based on our analysis in Theorem 4 and Appendix D.1, the main source of the approximation error is ρ , which mainly consists of two components: (1) the step size $\eta_{e,b}$ and (2) the maximum eigenvalue λ_1 of Hessian $\frac{1}{|\mathcal{B}_{e,b}|} \mathbf{H}_{e,b}$. Therefore, effectively reducing λ_1 during optimization, so that the training enters a flatter region, will not only improve the generalization ability of learned model but also reduce the approximation error in the unlearning stage. A possible approach is through sharpness-aware minimization [55, 56], which can effectively reduce λ_1 .

E.3 Online Unlearning-Repairing Strategy for Algorithm 1

While our approach does not require accessing any datasets in Stage III, we can mitigate the performance degradation caused by excessive deletions and make our algorithm more robust through a simple fine-tuning strategy if we can still access the remaining dataset in Stage III.

Specifically, when the continuous incoming deletion requests to forget data, we can rapidly implement certified unlearning through vector addition. This involves augmenting the current model with approximators, where errors accumulate during this process and thus cause performance degradation. Suppose, upon the arrival of a new round of deletion requests for a particular model and dataset, the model’s accuracy significantly drops due to the removal of a substantial amount of data. In such the scenario, we can address this performance degradation by fine-tuning the current model for E_r epochs on the remaining dataset, referred to as the ‘repairing’ process. Additionally, by computing the approximators for the remaining dataset during the repairing process, and adding these approximators

during the repairing process to the pre-stored approximators during the learning process, we obtain the new set of approximators for the remaining data.

Algorithm 2: Hessian-free Online Unlearning-Repairing Strategy

```

1 Stage I: Learning model  $\mathbf{w}_{E,B}$  on dataset  $S = \{z_i\}_{i=1}^n$ :
2 for  $e = 0, 1 \dots, E$  do
3   for  $b = 0, 1 \dots, B$  do
4     Compute gradient:  $\mathbf{g} \leftarrow \frac{1}{|\mathcal{B}_{e,b}|} \sum_{i \in \mathcal{B}_{e,b}} \nabla \ell(\mathbf{w}_{e,b}; z_i) \times \max(1, \frac{C}{\|\nabla \ell(\mathbf{w}_{e,b}; z_i)\|})$ ,
5     Gradient descent:  $\mathbf{w}_{e,b+1} \leftarrow \mathbf{w}_{e,b} - \eta_{e,b} \mathbf{g}$ 
6   end
7 end
8 Stage II: Pre-computing and Pre-storing statistics  $\mathcal{T}(S) = \{\mathbf{a}_{E,B}^{-u_j}\}_{j=1}^n$ :
9 for  $j = 1, 2 \dots, n$  do
10   Recursive computation by using HVP:  $\mathbf{a}_{E,B}^{-u_j} \leftarrow \sum_{e=1}^E \mathbf{M}_{e,b(u_j)} \nabla \ell(\mathbf{w}_{e,b(u_j)}; u_j)$ ,
11   where  $\mathbf{M}_{e,b(u_j)} = \frac{\eta_{e,b(u_j)}}{|\mathcal{B}_{e,b(u_j)}|} \prod_{k=e}^E \prod_{b=b(u_j)+1}^{B-1} (\mathbf{I} - \frac{\eta_{k,b}}{|\mathcal{B}_{k,b}|} \mathbf{H}_{k,b})$ 
12 end
13 Stage III: Unlearning when user requests to forget the subset  $U = \{u_j\}_{j=1}^m$  on model  $\mathbf{w}_{E,B}$ :
14 Compute:  $\bar{\mathbf{w}}_{E,B}^{-U} \leftarrow \mathbf{w}_{E,B} + \mathbf{a}_{E,B}^{-U}$ ,  $c \leftarrow 2\eta C \frac{\sqrt{2\ln(1.25/\delta)}}{\epsilon} \zeta_T^{-U}$  Delete statistics:  $\{\mathbf{a}_{E,B}^{-u_j}\}_{j=1}^m$ 
15 Sample:  $\sigma \sim \mathcal{N}(0, c\mathbf{I})$ , Return:  $\tilde{\mathbf{w}}_{E,B}^{-U} = \bar{\mathbf{w}}_{E,B}^{-U} + \sigma$ 
16 Repairing (Fine-tuning) the model  $\tilde{\mathbf{w}}_{E,B}^{-U}$  on the remaining dataset  $S \setminus U = \{z_r\}_{r=1}^{n-m}$ :
17 for  $e = 0, \dots, E_r$  do
18   for  $b = 0, 1 \dots, B$  do
19     Compute gradient:  $\mathbf{g} \leftarrow \frac{1}{|\mathcal{B}_{e,b}|} \sum_{r \in \mathcal{B}_{e,b}} \nabla \ell(\mathbf{w}_{e,b}; z_r) \times \max(1, \frac{C}{\|\nabla \ell(\mathbf{w}_{e,b}; z_r)\|})$ ,
20     Gradient descent:  $\mathbf{w}_{e,b+1} \leftarrow \mathbf{w}_{e,b} - \eta_{e,b} \mathbf{g}$ 
21   end
22 end
23 Pre-computing statistics  $\mathcal{T}(S) = \{\mathbf{a}_{E,B}^{-u_r}\}_{r=1}^{n-m}$  of the remaining dataset  $S \setminus U = \{z_r\}_{r=1}^{n-m}$ :
24 for  $r = 1, 2 \dots, n - m$  do
25   Recursive computation by using HVP:
26    $\mathbf{a}_{E+E_r,B}^{-u_r} \leftarrow \mathbf{M}_{e,b(u_r)} \mathbf{a}_{E,B}^{-u_r} + \sum_{e=1}^{E_r} \mathbf{M}_{e,b(u_r)} \nabla \ell(\mathbf{w}_{e,b(u_r)}; u_r)$ 
27   where:  $\mathbf{M}_{e,b(u_r)} = \frac{\eta_{e,b(u_r)}}{|\mathcal{B}_{e,b(u_r)}|} \prod_{k=e}^{E_r} \prod_{b=b(u_r)+1}^{B-1} (\mathbf{I} - \frac{\eta_{k,b}}{|\mathcal{B}_{k,b}|} \mathbf{H}_{k,b})$ 
28 end

```

E.4 Social Impacts

This paper introduces a Hessian-free online unlearning method via maintaining a statistical vector for each data sample, computed through affine stochastic recursion approximation of the difference in the retrained and the unlearn models. We have shown that our approach outperforms the existing results in terms of time/memory costs, while also enhancing generalization. While the unlearning algorithm was initially proposed to assist organizations in complying with data protection regulations (e.g., GDPR) and help build trust in AI systems by demonstrating the ability to correct mistakes or biases, it is important to be mindful of potential negative consequences: Unlearning algorithms can introduce unforeseen biases or inaccuracies in subsequent predictions or decisions. In addition, adversarial actors could potentially exploit machine unlearning processes to manipulate or subvert models.